Summer 8-31-2002

Quantitative assessment of reflex blood pressure regulation using a dynamic model of the cardiovascular system

Tanha Patel
New Jersey Institute of Technology

ABSTRACT

QUANTITATIVE ASSESSMENT OF REFLEX BLOOD PRESSURE REGULATION USING A DYNAMIC MODEL OF THE CARDIOVASCULAR SYSTEM

by
Tanha Patel

A quantitative understanding of the changes in coronary, pulmonary and systemic hemodynamic variables and their effects on the regulation mechanism is important to the better postoperative management of patients with impaired cardiac function. The arterial baroreflex plays a key role in blood pressure homeostasis, and its impairment may result in exaggerated blood pressure fluctuations and an increased risk of cardiovascular morbid events.

The objective of this work was to construct a mathematical model of the cardiovascular system, which will allow us to simulate the effects of the baroreceptor reflex regulation on sudden changes in blood pressure, caused by sudden changes in one or more hemodynamic parameters. These parameters include heart rate, peripheral resistance and ventricular contractility. A comprehensive model of the baroreflex-feedback mechanism regulating the heart rate, the contractility of the ventricle and the peripheral vascular resistance is presented. The model used is a combination of several models, which have been reported in literature, along with our own modifications. The important feature of the model is that it is dynamic in nature and thus it is helpful in real time analysis. The model is also useful to conceptualize the problem and test relationships, helping researchers frame hypotheses and design experiments.

QUANTITATIVE ASSESSMENT OF REFLEX BLOOD PRESSURE REGULATION USING A DYNAMIC MODEL OF THE CARDIOVASCULAR SYSTEM

by
Tanha Patel

A Thesis
Submitted to the Faculty of
New Jersey Institute of Technology
in Partial Fulfillment of the Requirements for the Degree of
Master of Science in Biomedical Engineering

Department of Biomedical Engineering

August 2002

APPROVAL PAGE

QUANTITATIVE ASSESSMENT
OF REFLEX BLOOD PRESSURE REGULATION
USING A DYNAMIC MODEL OF THE CARDIOVASCULAR SYSTEM

Tanha Patel

8/5/02

Dr. Arthur Ritter, Thesis Advisor — Date
Professor of Pharmacology and Physiology, UMDNJ

8/5/02

Dr. David Kristol, Committee Member — Date
Associate Chair and Professor of Biomedical Engineering, NJIT

08/05/02

Professor Peter Engler, Committee Member — Date
Emeritus Professor of Biomedical Engineering, NJIT

BIOGRAPHICAL SKETCH

Author: Tanha Patel

Degree: Master of Science

Date: August 2002

Date of Birth:

Place of Birth:

Undergraduate and Graduate Education:

- Master of Science in Biomedical Engineering,
  New Jersey Institute of Technology, Newark, NJ, 2002

- Bachelor of Science in Biomedical Engineering,
  D. J. Sanghvi College of Engineering, Mumbai, India, 2000

Major: Biomedical Engineering

To

MY PARENTS
For Their Love and Patience

MY SISTERS
For Their Care

MY FRIENDS: Alok and Suhrud
For Their Abundant Support, for Their Care and Understanding

ACKNOWLEDGMENT

I would like to express my deepest appreciation to Dr. Arthur Ritter, for his patience and wisdom, throughout the length of this study and the preparation of this thesis, and without whose guidance this thesis would not have been possible. Special thanks to Dr. David Kristol and Prof. Peter Engler for serving as members of the committee.

I am also grateful to Dr. David Kristol and the Biomedical Engineering Department for extending financial support for this thesis.

Thank you, Alok, for all you have done. From your heart, you share so much goodness. I also wish to thank Suhrud for always standing by me all these years.

TABLE OF CONTENTS

TABLE OF CONTENTS
(Continued)

Chapter **Page**

LIST OF TABLES

LIST OF FIGURES

LIST OF FIGURES
(Continued)

Figure **Page**

CHAPTER 1

INTRODUCTION

1.1. Objective

Transport of blood through the body is well regulated. The heart and large arteries form a system in which blood pressure is maintained. This helps to have a continuous pool of blood with sufficient pressure head from which the organs can derive blood at a rate sufficient to sustain their function. The need of an organ for blood flow is not constant but depends on its function at a certain point in time. The heart is directed by a cleverly designed system of feedback, feed forward and anticipating regulatory processes which instruct the heart, when to work harder or not so hard to maintain the pressure in the vascular vessels within limits. The body uses the nervous system to maintain some control over the distribution of flow to the different organs. If all the organs were provided maximal flow at the same time, the heart would not be able to sustain the effort. The circulation can go out of control, for example in circulatory shock, a doctor's nightmare in the intensive care unit.

In order to optimize the flows so that all the cells get what they need under general circumstances, several control mechanisms interact. The result is heterogeneity in the distribution of blood flows. Under conditions of increased need for blood flow or under circumstances of disease resulting in additional restrictions to blood flow due to, for example atherosclerosis, there will be local areas at risk. The ultimate danger is cell death and necrosis so that when there is competition among control mechanisms, local control prevails. The system for control of the vasculature is one that cannot be readily

understood without integrating one's knowledge of the many components contributing to that control. A quantitative approach to this is through mathematical modeling.

Many aspects of the structure and function of the cardiovascular system can be described and analyzed in mathematical terms. The anatomy of the cardiovascular system and the hydraulic principles that govern the movement of blood within the system are relatively well understood. The diagnosis and treatment of cardiovascular disease may be improved by using mathematical models. Mathematical modeling can extrapolate from known states to those projected states that cannot be measured directly and approximate those variables that are inaccessible to experiment. On the other hand, mathematical modeling is a flexible tool allowing change of parameters and control of variables while reducing animal and human experimentation. Without models, the only development of treatment is by trial and error, where error probably means a shorter life or lower quality of life for the patient involved.

In the present study, a mathematical model of the closed-loop cardiovascular system was devised. Baroreceptor reflex control of blood pressure was incorporated into the model. The model was used to study the response of baroreceptor reflexes to parameter changes in the closed-loop circulation.

1.2 Physiology of Cardiovascular Circulation

The overall functional arrangement of the cardiovascular system is illustrated in Figure 1.1. The cardiovascular system is made up of a pump (the heart), a series of distributing and collecting tubes (the arteries and veins), and an extensive system of thin-walled blood

vessels that permit the rapid exchange of substances between tissues and the vascular channels (the capillaries). Since a functional rather than an anatomic viewpoint is expressed in the figure, the heart appears in two places: the right heart pump and the left heart pump. Each pump has two chambers, an atrium and a ventricle, connected by one-way valves, called atrioventricular (AV) valves. The AV valves are designed so that blood can flow only in one direction, from the atrium to the ventricle.

The right and the left hearts have different functions. The right heart, the pulmonary arteries, capillaries, and the veins are collectively called the pulmonary circulation. The right ventricle pumps blood to the lungs. The left heart, the systemic arteries, capillaries and the veins are collectively called the systemic circulation. The left ventricle pumps blood to all organs of the body, except the lungs. The right heart and the left heart function in series so that the blood is pumped sequentially from the right heart to the pulmonary circulation, to the left heart, to the systemic circulation, and then back to the right heart.

Blood that has been oxygenated in the lungs returns to the left atrium via the pulmonary vein. This blood then flows from the left atrium to the left ventricle through the mitral valve (the AV valve of the left heart). Blood leaves the left ventricle through the aortic valve, which is located between the left ventricle and the aorta. When the left ventricle contracts, the pressure in the ventricle increases, causing the aortic valve to open and blood to be ejected forcefully into the aorta. Blood then flows through the arterial system, driven by the pressure created by the contraction of the left ventricle. The total cardiac output of the left heart is distributed among the organ systems via sets of parallel arteries. The blood leaving the organs is venous blood that is collected in veins of

increasing size and finally in the largest vein, the vena cava. The vena cava carries blood to the right heart.

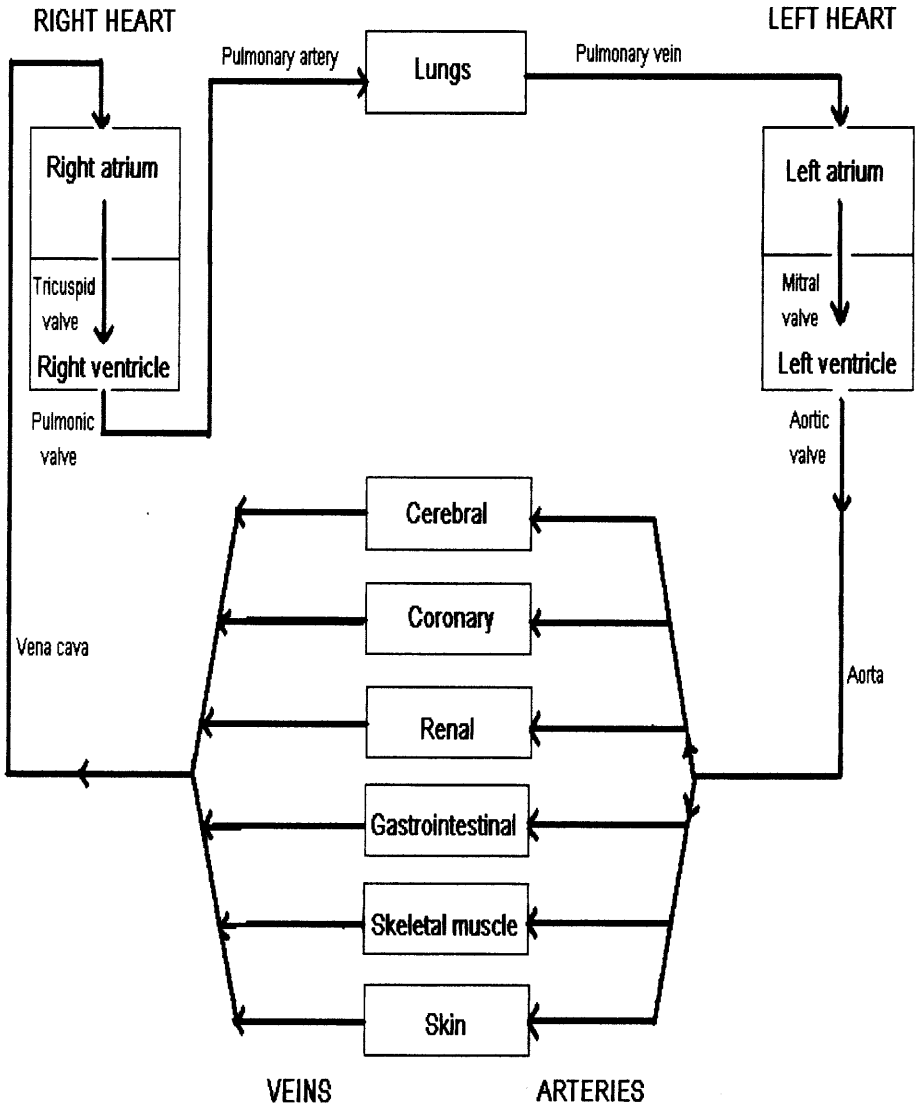

Figure 1.1 A schematic diagram showing the circuitry of the cardiovascular system. The arrows show the direction of blood flow.

The blood from the left heart flows rapidly through the aorta and the systemic arteries. Since the arteries have large diameter, they serve as low-resistance tubes conducting blood to the various organs. Their second major function is to act as a "pressure reservoir" for maintaining blood flow through the tissues during diastole. From the aorta to the arteries, the frictional resistance to blood flow as well as the pressure drop is relatively low. The arterioles are the principal points of resistance in the cardiovascular system that can be illustrated by considerable amount of pressure drop from the arterioles to the capillaries (Figure 1.2).

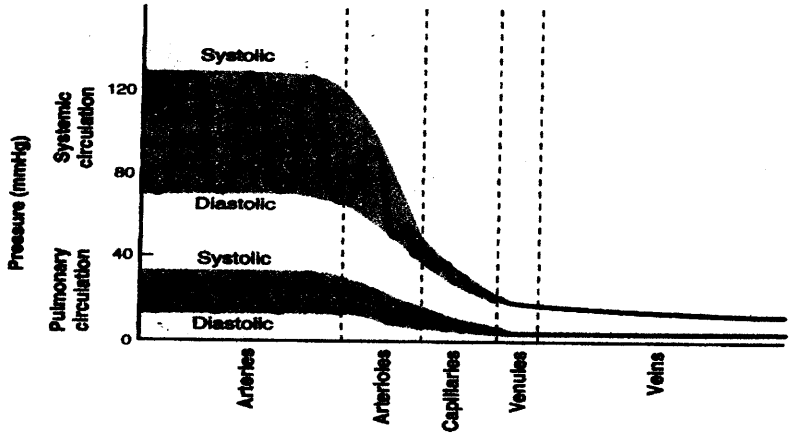

Figure 1.2 Pressures in the vascular system.

The blood velocity, very high in the aorta, slows progressively in the arteries and arterioles and then slows markedly as it passes through the huge cross-sectional area of the capillaries. The velocity of flow then progressively increases in the venules and veins due to decrease in the cross-sectional area. The veins are the last set of tubes through which blood flows on its way back to the right heart. In the systemic circulation, the force driving this venous return is the pressure difference between the peripheral veins and the right atrium. The pressure in the first portion of the peripheral veins is generally quite low

because resistance dissipates most of the pressure imparted to the blood by the heart as the blood flows through the arteries, capillaries, and venules. The pressure difference is adequate because of the low resistance to flow offered by the veins, which have large diameters. Thus, a major function of the veins is to act as low-resistance conduits for blood flow from the tissue to the heart. The walls of the veins are thin and very compliant making it capable of accommodating large volumes of blood with a relatively small increase in internal pressure. Most of the blood (about 67% of the total blood volume at rest) in the systemic circulation is contained in the venous vessels.

The arterioles play two major roles: (1) they are a major factor in determining mean arterial pressure, and (2) the arterioles in individual organs are responsible for determining the relative blood-flow distribution to those organs. Appropriate systemic arterial pressure is perhaps the single most important requirement for proper operation of the cardiovascular system. The peripheral circulation is essentially under dual control: centrally by the nervous system, and locally in the tissues by the conditions in the immediate vicinity of the blood vessels. The relative importance of these two mechanisms is not the same in all the tissues. In some areas of the body, such as the skin and the splanchnic regions, neural regulation of blood flow predominates, whereas in others, such as the heart and the brain, local control is dominant. The term local control denotes mechanisms independent of nerves or hormones by which organs and tissues alter their own arteriolar resistances, thereby, self-regulating their blood flow. This self-regulation is termed as autoregulation.

The arterioles that control flow through a given organ or tissue lie within the organ tissue itself. Thus, arterioles and the smooth muscle in their walls are exposed to

the chemical composition of the interstitial fluid of the organ they serve. The interstitial concentrations of many substances reflect the balance between the metabolic activity of the tissue and its blood supply. Interstitial oxygen levels, for example, fall whenever the tissue cells are utilizing oxygen faster than it is being supplied to the tissue by blood flow. Conversely, interstitial oxygen levels rise whenever excess oxygen is being delivered to a tissue from the blood. In nearly all the vascular beds, exposure to low oxygen reduces arteriolar tone and causes vasodilation, whereas high oxygen levels cause arteriolar vasoconstriction. Thus, a local feedback mechanism exists that automatically operates on arterioles to regulate a tissue's blood flow in accordance to its oxygen demands, the oxygen levels around arterioles fall, the arterioles dilate, and the blood flow through the organ appropriately increases.

Without sufficient arterial pressure, the brain and the heart do not receive adequate blood flow no matter what adjustments are made in the vascular resistance by local control mechanisms. Various sensors located within the body continuously monitor arterial pressure. Whenever arterial pressure varies from normal, multiple reflex responses are initiated which cause the adjustments in cardiac output and total peripheral resistance needed to return arterial pressure to its normal value. In the short term (within 1-2 heart beats), these adjustments are brought about by changes in the activity of the autonomic nerves leading to the heart and the peripheral vessels. In the long term (minutes to days), other mechanisms such as changes in the cardiac output brought about by changes in the blood volume (through renal mechanisms) play an increasingly important role in the control of arterial pressure.

The arterial baroreceptor reflex is the most important mechanism providing short-term regulation of arterial pressure. The baroreceptor mechanisms are fast, neurally mediated reflexes that attempt to keep arterial pressure constant via changes in the output of the sympathetic and parasympathetic nervous systems to the heart and blood vessels. Stretch sensors, the baroreceptors, are located within the walls of the carotid sinus and the aortic arch and relay information about blood pressure to cardiovascular vasomotor centers in the brain stem. The carotid sinus baroreceptors are responsive to increases or decreases in arterial pressure, whereas the aortic arch baroreceptors are primarily responsive to increases in arterial pressure. The baroreceptors are mechanoreceptors, which are sensitive to pressure or stretch. Increases in arterial pressure cause increased stretch on the baroreceptors and increased firing rate in afferent nerves that travel to the brain stem. Decreases in arterial pressure cause decreased stretch on the baroreceptors and decreased firing rate in the afferent nerves. An increase in arterial pressure directs the medullary cardiovascular centers to increase the parasympathetic outflow to the heart and a decrease in sympathetic outflow to the heart and blood vessels. This change in the parasympathetic and sympathetic outflow results in a decrease in the heart rate, cardiac contractility and total peripheral resistance. All these factors contribute to the reduction in arterial pressure to a new steady state depending on the pathology of the individual involved. A stimulus of decreased arterial pressure would elicit events exactly opposite to those just described and produce the response of increased arterial pressure.

1.3 History of Mathematical Model of Cardiovascular System

Earlier works in the modeling of the cardiovascular system focused mainly on hemodynamics in the major arteries. One of the themes was to represent the different elements of the system as elastic reservoirs, i.e., Windkessels. A Windkessel compartment is described by a single ordinary first-order differential equation. The pressure P in the compartment is related to the compartment's volume V by a compliance term C ($P = V/C$). The change in volume is equal to the difference of inflow F_I and outflow F_0 ($dV/dt = F_I - F_0$). The ventricle was thought of as a Windkessel with time-varying compliance.

In 1955, Guyton described a graphic method of cardiac output determination in which venous return and cardiac output, both as functions of right atrial pressure, are equated. Grodins (1959) developed a systematic mathematical approach to the cardiovascular system. He published one of the first mathematical models of the complete or closed circulatory system. Six compartments were defined corresponding to those shown in Figure 1.3. He used the Starling's "law of the heart" assuming external stroke work to be directly proportional to end-diastolic ventricular volume. Solution of 23 independent equations yields mean values of variables that are in agreement with results of physiologic experiments.

Warner (1959) described the closed circulatory system with 18 equations. Defares et al. (1963) worked out a description of the uncontrolled circulatory system. The time courses of the ventricular compliances have been derived from the ventricular function curves and ventricular outflow-time curves. Homeometric autoregulation (Sarnoff et al., 1960) was also incorporated. Dick and Rideout (1965) described an analog computer

model of the arterial tree having four arterial sections and a time varying compliance of the left ventricle.

In 1967, Guyton and Coleman presented a model of the circulation, which included cardiovascular control mechanisms. Cardiac output was determined by the strength of the heart, vascular resistance and blood volume. Vascular resistance was determined by autoregulation of blood flow with above-normal cardiac output causing vasoconstriction and below-normal cardiac output causing vasodilatation. The baroreflexes were included but they had only a short-term effect on the circulation.

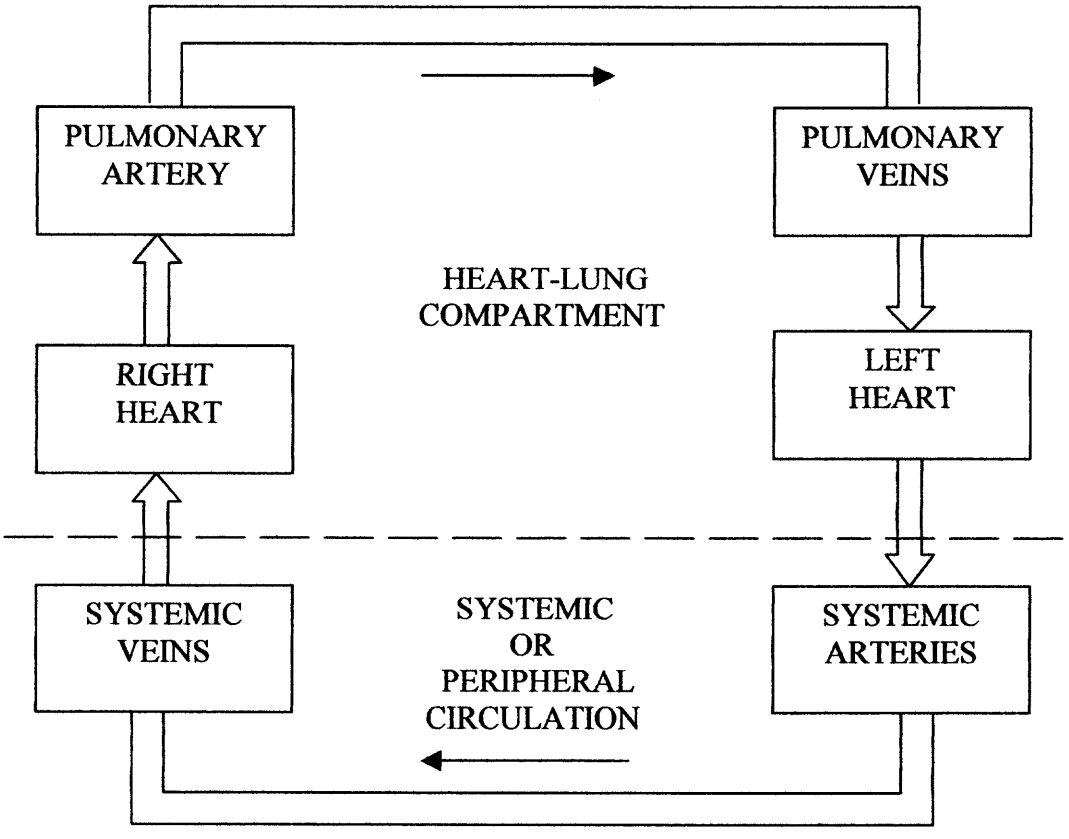

Figure 1.3 A six-compartment model of the closed circulatory system

In 1979, Coleman described a model that combined detailed cardiovascular functions with many interacting physiological processes including the lungs, control of respiration, transport and exchange of blood gases, fluid shifts, kidney function, baroreflexes, acid-balance, and skeletal muscle mechanics.

At present, there are many published models of the cardiovascular system. Different models are used in different research projects depending on their objective.

CHAPTER 2

CARDIOVASCULAR SYSTEM MODEL

2.1. The Computer Model

To formulate a model of the cardiovascular system, the system has been divided into twenty compartments corresponding to the major anatomic components: the Left ventricle, Aorta, Large Arteries (I, II, III), Arterioles, Systemic Capillaries, Venules, Large Veins, Vena Cava, Right Ventricle, Pulmonary Arterial System, Pulmonary Capillary System, Pulmonary Venous System along with the Coronary circulation, Brain, Kidneys, Hepatic Artery, Liver, Spleen and GI Tract, and a Skeletal Muscle compartment. For the last five compartments, capillaries are omitted and their venules are lumped into the Large Vein compartment. Characteristic resistance (R) and compliance (C) given by the two-element Windkessel model represent each of the compartments. Figure 2.1 shows a schematic of the circulatory system.

The basic resistance equation states that pressure drop between compartments are a function of the flow and the resistance to flow between the compartments. The basic equation that states its relationship, between any two compartments (e.g. i and $i+1$) is:

$$P_i - P_{i+1} = F_i \times R_{i+1} \tag{2.1}$$

where P_i and P_{i+1} are the blood pressures in the compartments i and $i+1$. Compartment i is upstream of compartment $i+1$. F_i is the blood flow out of compartment i and into compartment $i+1$. R_{i+1} is the vessel resistance of compartment $i+1$. This well known relationship between flow, pressure, and resistance is analogous to the relationship between current, voltage, and resistance in electrical circuits, as expressed by Ohm's law.

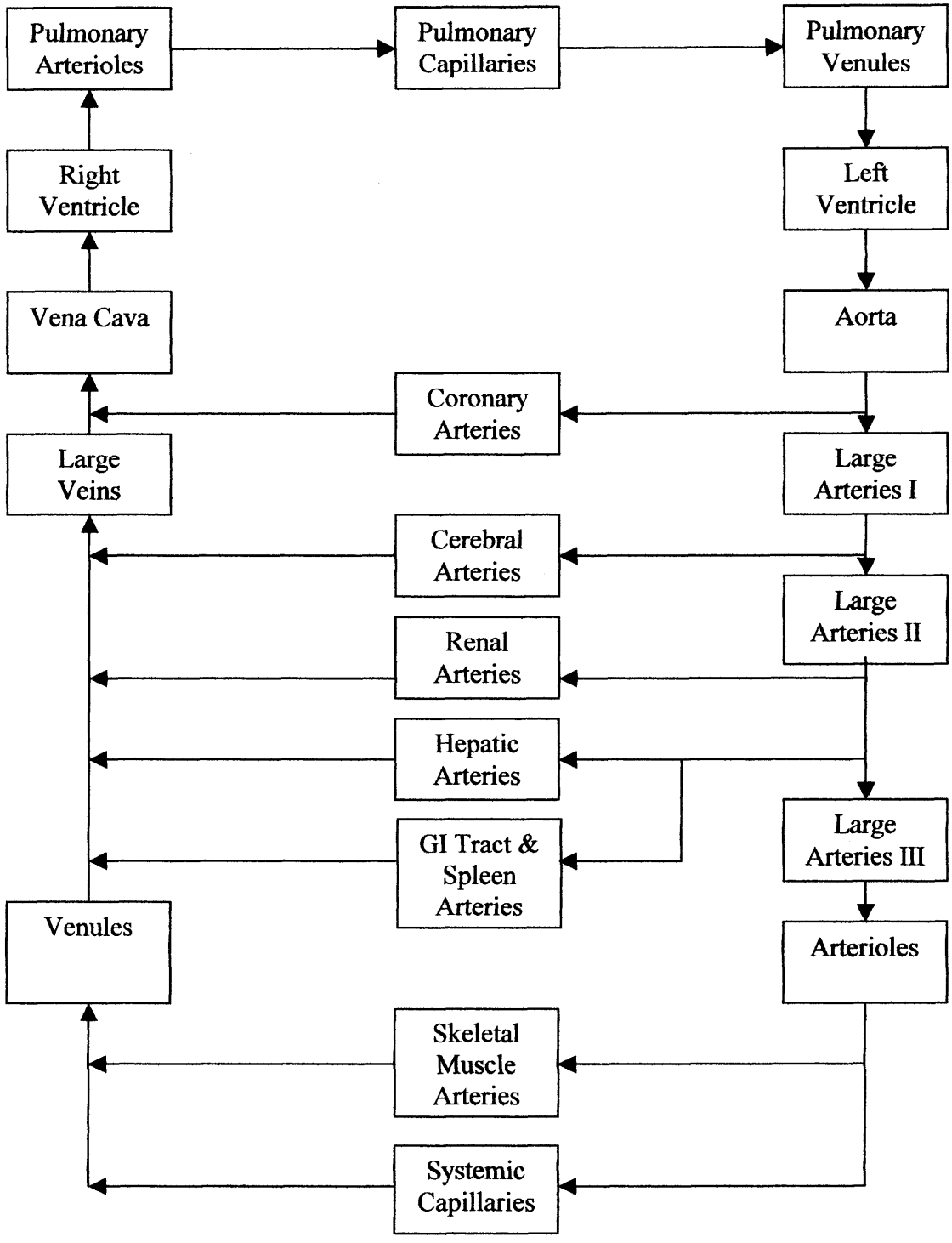

Figure 2.1 Schematic diagram of the closed loop model of the cardiovascular system used in this work.

The composite radius of the vessels primarily determines the resistance, although changes in viscosity of the blood will also alter the resistance. It is necessary to consider each vascular bed separately. Within each bed, the arteriolar, postcapillary, and venous resistances are in series and can be added to obtain the total resistance in that bed. Thus, these equations determine the pressures in all compartments of the circulation relative to the pressures in the adjacent compartments. They do not determine the absolute transmural pressure in any compartment. This is determined by the compliance equations. The above equations refer to a static circulatory system, i.e. the pressures are not varying with time. A dynamic system is realized if the pressures and flows vary with time:

$$\frac{dP_i}{dt} - \frac{dP_{i+1}}{dt} = \frac{dF}{dt} \times R \tag{2.2}$$

where P, F and R represent the same as above.

Within each compartment, transmural pressure is a function of the blood volume in the compartment and the compliance of its walls:

$$P_i = (V_i - V_{0i}) / C_i : \quad for\ V_i < V_{0i};\quad P_i = 0 \tag{2.3}$$

where C_i is the compliance of the compartment i. V_i is the blood volume of the compartment i. V_{0i} is the unstressed volume which is the maximum achievable volume with an internal pressure of zero in compartment i. Unstressed volume is particularly important on the venous side of the circulation where over one-half of a vein's normal volume is the unstressed volume. According to Equation (2.3), the dynamic relationship of volume and pressure is described by Equation (2.4):

$$\frac{dP_i}{dt} = \frac{(dV_i / dt)}{C_i} \tag{2.4}$$

This equation assumes a linear relation between volume and pressure, with the volume decreasing to zero when the pressure is zero. Other models have assumed a finite volume of blood in the circulation at zero pressure. However, this volume cannot be measured accurately and it changes; therefore equations of this type will be very complex. Therefore, equations as simple as possible were used in this analysis.

According to the law of conservation of mass, Equation (2.5) describes the variation of blood volume in compartment *i*:

$$dV_i/dt = F_{in} - F_{out} \tag{2.5}$$

where F_{in} is the blood flow into the compartment *i* and F_{out} is the blood flow out of the compartment *i*. The elastance (reciprocal of compliance) of the heart was made to change periodically in accordance with a set of pre-chosen values. Modelers of the circulatory system in simulating the ventricular pump performance have often used a similar concept of time-varying elastance. This analysis adopts the time-varying elastance concept from Suga and Sagawa's [1] work. The following section gives a brief validation for the use of the time-varying elastance in the present model.

2.2 Time Varying Pressure-Volume Ratio

In Suga's study [1], they used the time-varying ratio of pressure to volume at any instant to represent the pressure-volume relationship of the left ventricle in the dog. The ratio was defined as the elastance of a ventricle *E(t)* (*E(t) = P(t) / V(t)*). The mean *E(t)* curve and the standard deviation from a set of five to ten consecutive beats under each loading condition for each contractile state was computed [1]. This output was recorded on an x-y

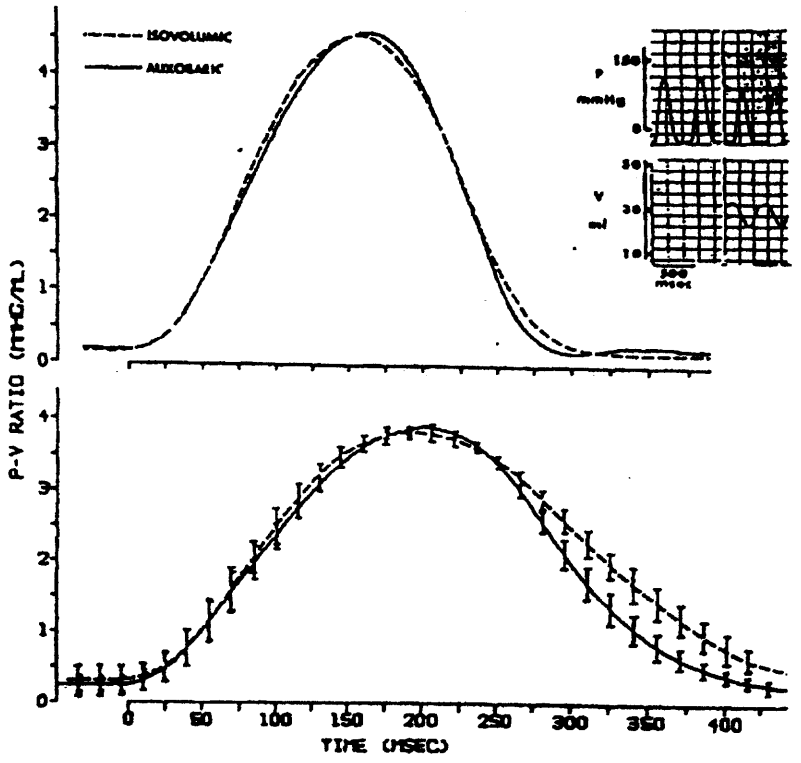

Figure 2.2 Two examples of superimposed tracings of the time-varying pressure-volume ratio. *E(t)*, of the left ventricle contracting auxobarically and isovolumically for the control contractile state. Top: Mean *E(t)* curves from six consecutive beats contracting with the same end-diastolic volume in one ventricle. The insert shows the raw pressure and volume tracings from which the corresponding *E(t)* curves were obtained by computer. Bottom: Two mean *E(t)* curves, each of which is a mean of five mean *E(t)* curves obtained from differently preloaded beats in one ventricle of another dog. The vertical bars indicate standard deviation.

plotter. The pressure-volume ratio curves obtained for a given contractile state were similar in contour and magnitude regardless of the difference in the loading conditions. The top of Figure 2.2 shows examples of the computer generated mean *E(t)* curves, one from isovolumic beats and the other from auxobaric beats [1]. The bottom of the figure shows examples of the means of the mean *E(t)* curves acquired under the different loading conditions and a constant contractile state in one heart. As the curves indicate, there was little difference between the isovolumic and auxobaric (increase in pressure)

E(t) curves at any time in systole. The diastolic phase of the curve in auxobaric contractions was situated slightly lower than that in isovolumic ones. *E(t)* can be characterized by E_{max} (the peak value of the pressure-volume ratio curve) and T_{max} (the time to E_{max} from the onset of systole). Statistical analysis showed that E_{max} was unaffected by the changes in loading condition (standard deviation of the mean E_{max} in a given preparation was 3-4%). Moreover, T_{max} was not affected by the changes in end-diastolic volume (standard deviation of the mean T_{max} in a given ventricle was about 6%). T_{max}, however, was slightly prolonged with the change of the contraction mode from isovolumic to auxobaric. These findings were common to both the control and the enhanced contractile state.

The results of their study demonstrated that *E(t)* adequately represents the instantaneous pressure-volume relationship of the left ventricle in systole. The load-independence and the similarity of the basic shape of *E(t)* curve seems to be a fundamental feature of ventricular contraction. The contractility of the ventricle can be fully represented by two parameters, E_{max} and T_{max}. Therefore, the pressure-volume relationship of the left ventricle in the present model is represented as follows:

$$P_{lv}(t) = E_{lv}(t)\left[V_{lv}(t) - V_{lv0}\right] \tag{2.6}$$

where $E_{lv}(t)$ is the elastance of the left ventricle. V_{lv0} is the volume axis intercept of the line connecting the maximum left ventricular elastance P/V points for different loaded beats and was confirmed experimentally to be a constant. $E_{lv}(t)$ can be expressed as in Equation (2.7).

$$E_{lv}(t) = E_{l\max} E_n\left(t/T_{\max}\right) \tag{2.7}$$

where E_{lmax} is the maximum value of $E_{lv}(t)$. $E_n(t)$ is the normalized elastance (i.e. the maximum of $E_n(t) = E_n(1) = 1$). $E_n(t)$ is represented by a third-order polynomial approximation as follows:

$$E_n(t) = a_1 t + a_2 t^2 + a_3 t^3 \tag{2.8}$$

where the coefficients a_1, a_2, and a_3 can be obtained by using the least square method. In the present model, $E_n(t)$ is based on the normalized function used by Shroff et al. [2] and Barnea et al. [3]. The coefficients are given as follow:

$$a_1 = 0.158; \quad a_2 = 2.685; \quad a_3 = -1.841$$

T_{max} is the time at which the $E_{lv}(t)$ reaches the maximum value E_{max} from the onset of systole. It can be calculated as follows [3]:

$$T_{\max} = (413 - 1.7 \times HR)/1000 \tag{2.9}$$

where HR is in beats per minute. T_{max} is in seconds.

The right ventricle model is similar to the left ventricle model, but has a different elastance $E_{rv}(t)$. In this study, the same normalized elastance as in the left ventricle is used. Therefore, the pressure-volume relationship is represented as follows:

$$E_{rv}(t) = E_{r\max} E_n(t/T_{\max}) [V_{rv}(t) - V_{rv0}] \tag{2.10}$$

where E_{rmax} is the elastance of the right ventricle and has a different value than the left ventricle. Generally, E_{rmax} is about one-fifth of E_{lmax}. V_{rv0} is the volume axis intercept of the line connecting the maximum right ventricular elastance P/V points for different loaded beats. Unlike the left ventricle, V_{rv0} varies continuously throughout the cardiac cycle. In this model, V_{rv0} is assumed to be constant.

In diastole, the compliance of the ventricles is assumed to be constant, but the left ventricle and right ventricle have different values.

2.3 Model Equations

Each compartment in the model is described using Equations (2.1) to (2.4). The parameters and variables for each compartment as used in various literatures are given in Table 2.1. The following equations are used to describe the model of the circulatory system and form the basis of the simulation.

Left Ventricle:

$$d(VLV)/dt = FVP - FLV$$
$$FVP = 50\,(PVP - PLV) \quad FVP = 0; \quad for PLV > PVP$$
$$FLV = 50\,(PLV - PAO) \quad FLV = 0; \quad for PAO > PLV$$
$$PLV = E_{lv}(t) \times VLV$$

where VLV is the volume of the Left Ventricle. FVP and FLV are the flows from the Pulmonary Venules to the Left Ventricle and from the Left Ventricle to the Aorta, respectively. PVP, PLV and PAO are the pressures in the Pulmonary Venules, Left Ventricle, and Aorta, respectively. To represent the closing of the mitral valve, FVP is set to zero when $PLV > PVP$. To represent the closing of the aortic valve, FLV is set to zero when $PAO > PLV$. $E_{lv}(t)$ is the elastance of the Left Ventricle. In systole, $E_{lv}(t) = 2\,E_n(t)$. $E(t)$ is calculated by Equation (2.7) and (2.8). In diastole, $E_{lv}(t) = 0.051$.

Aorta:

$$d(VAO)/dt = FLV - FAO - FCOR$$
$$FAO = 10.5882\,(PAO - PLAI)$$
$$PAO = (VAO - 60)\,/\,0.625$$

where VAO is the volume of the Aorta. FAO and $FCOR$ are the flows out of the Aorta into the Large Arteries I and from the Aorta to the Coronary Artery, respectively. The

flow from the Aorta to the Coronary Artery is controlled by autoregulation of the Coronary Artery. *PLAI* is the pressure in the Large Arteries I.

Large Arteries I:

$$d(VLAI)/dt = FAO - FCER - FLAI$$
$$FLAI = 7.6491\,(PLAI - PLAII)$$
$$PLAI = (VLAI - 58)/0.725$$

where *VLAI* is the volume of the Large Arteries I. *FCER* and *FLAI* are the flows from the Large Arteries I to the Cerebral Arteries and from the Large Arteries I to the Large Arteries II, respectively. *FCER* is controlled by autoregulation of the Cerebral Artery. *PLAII* is the pressure in the Large Arteries II.

Large Arteries II:

$$d(VLAII)/dt = FLAI - FREN - FSGI - FHEP - FLAII$$
$$FLAII = 5.8824\,(PLAII - PLAIII)$$
$$PLAII = (VLAII - 70)/1$$

where *VLAII* is the volume of the Large Arteries II. *FREN*, *FSGI*, *FHEP*, and *FLAII* are the flows from the Large Arteries II to the Renal Arteries, from the Large Arteries II to the Spleen and the GI Tract, from the Large Arteries II to the Hepatic Artery, and from the Large Arteries II to the Large Arteries III, respectively. *FREN*, *FSGI* and *FHEP* are controlled by autoregulation of the Renal, Spleen and GI Tract, and Hepatic Arteries respectively. *PLAIII* is the pressure in the Large Arteries III.

Table 2.1 Standard Values of Variables and Parameters

(For a normal human heart at rest)

	Resistance (mm Hg/ml/sec)	**Compliance (ml/mm Hg)**	**Unstressed volume (ml)**
Left Ventricle	0.02		
Aorta	0.02	0.625	60
Large Arteries I	0.0944	0.725	58
Large Arteries II	0.1308	1	70
Large Arteries III	0.17	1	75
Arterioles	0.85	1.6667	53
Systemic Capillaries	0.85	15	171
Venules	0.0567	20.5	278
Large Veins	0.0057	121.5	1587
Vena Cava	0.0283	21.5	197
Right Ventricle	0.0069		
Pulmonary Arterioles	0.0333	5	88
Pulmonary Capillaries	0.025	4.44	68
Pulmonary Venules	0.02	7.9	147
Heart Rate (beats/min)	75		
E_{lmax} (mm Hg/ml)	2		
E_{rmax} (mm Hg/ml)	0.45		
V_{lv0} (ml)	0		
V_{rv0} (ml)	10		

Large Arteries III:

$$d(VLAIII)/dt = FLAII - FLAIII$$
$$FAA = 1.1765\,(PLAIII - PAA)$$
$$PLAIII = (VLAIII - 75)/1$$

where *VLAIII* is the volume of the Large Arteries III. *FLAIII* is the flow from the Large Arteries III to the Arterioles. *PAA* is the pressure in the Arterioles.

Arterioles:

$$d(VLAIII)/dt = FLAIII - FSM - FAA$$
$$FAA = 1.1765\,(PAA - PSC)$$
$$PAA = (VAA - 53)/1.6667$$

where *VAA* is the volume of the Arterioles. *FSM* and *FAA* are the flows from the Arterioles to the Skeletal Muscle and flow from the Arterioles to the Systemic Capillaries, respectively. *FSM* is controlled by autoregulation of the Skeletal Muscle Arteries. *PSC* is the pressure in the Systemic Capillaries.

Systemic Capillaries:

$$d(VSC)/dt = FAA - FSC$$
$$FSC = 17.647\,(PSC - PVU)$$
$$PSC = (VSC - 171)/15$$

where *VSC* is the volume of the Systemic Capillaries. *FSC* is the flow from the Systemic Capillaries to the Venules. *PVU* is the pressure in the Venules.

Venules:

$$d(VVU)/dt = FSC + FSM - FVU$$
$$FVU = 176.471\,(PVU - PLVE)$$
$$PVU = (VVU - 278)/20.5$$

where *VVU* is the volume of the Venules. *FVU* is the flow from the Venules to the Large Veins. *PLVE* is the pressure in the Large Veins.

Large Veins:

$$d(VLVE)/dt = FVU + FCER + FREN + FSGI + FHEP - FLVE$$
$$FLVE = 135.294\,(PLVE - PVC)$$
$$PLVE = (VLVE - 1587)/121.5$$

where *VLVE* is the volume of the Large Veins. *FLVE* is the flow from the Large Veins to the Vena Cava. *PVC* is the pressure in the Vena Cava.

Vena Cava:

$$d(VVC)/dt = FLVE + FCOR - FVC$$
$$FVC = 145\,(PVC - PRV)$$
$$PVC = (VVC - 197)/21.5$$

where *VVC* is the volume of the Vena Cava. *FVC* is the flow from the Vena Cava to the Right Ventricle. *PRV* is the pressure in the Right Ventricle.

Right ventricle:

$$d(VRV)/dt = FVC - FRV$$
$$FVC = 145\,(PVC - PRV) \quad FVC = 0; \quad for\ PRV > PVC$$
$$FRV = 30(PRV - PAP) \quad FRV = 0; \quad for\ PAP > PRV$$
$$PRV = E_{rv}(t) \times VRV$$

where *VRV* is the volume of the Right Ventricle. *FRV* is the flow from the Right Ventricle to the Pulmonary Arteries. *PAP* is the pressure in the Pulmonary Arteries. *FVC* is set to zero when $PRV > PVC$ in order to represent the closing of the tricuspid valve. To represent the closing of the pulmonic valve, *FRV* is set to zero when $PAP > PRV$. $E_{rv}(t)$ is the elastance of the Right Ventricle. In systole, $E_{rv}(t) = 0.45E_n(t)$, and $E_{rv}(t) = 0.048$ in diastole.

Pulmonary Arteries:

$$d(VAP)/dt = FRV - FAP$$
$$FAP = 40\,(PAP - PCP)$$
$$PAP = (VAP - 88)/5$$

where *VAP* is the volume of the Pulmonary Arteries. *FAP* is the flow from the Pulmonary Arteries to the Pulmonary Capillaries. *PCP* is the pressure in the Pulmonary Capillaries.

Pulmonary capillaries:

$$d(VCP)/dt = FAP - FCP$$
$$FCP = 50\,(PCP - PVP)$$
$$PCP = (VCP - 68)/4.44$$

where *VCP* is the volume of the Pulmonary Capillaries. *FAP* is the flow from the Pulmonary Capillaries to the Pulmonary Venules. *PVP* is the pressure in the Pulmonary Venules.

Pulmonary Venules:

$$d(VVP)/dt = FCP - FVP$$
$$FVP = 50\,(PVP - PLV)$$
$$PVP = (VCP - 147)/7.9$$

where *VVP* is the volume of the Pulmonary Venules. *FVP* is the flow from the Pulmonary Venules to the Left Ventricle. *PLV* is the pressure in the Left Ventricle.

Thus, completes the closed loop representing the pressures, volumes, and flows in the circulatory system.

2.4 Simulink Simulation Language

In the last few years, Simulink has become the most widely used software package in academia and industry for modeling and simulating dynamical systems. It supports linear and nonlinear systems, modeled in continuous time, sampled time, or a hybrid of the two. Systems can also be multirate, i.e., have different parts that are sampled or updated at different rates.

Real time system behavior is usually represented by linear and nonlinear differential equations. The solutions of these equations are possible only by "continuous simulation", which can be realized by using Simulink. These solutions can describe the movements and energetics of all complex physiologic systems. For modeling, Simulink provides a Graphical User Interface (GUI) for building models as block diagrams, using click-and-drag mouse operations. With this interface, you can draw the models just as you would with pencil and paper. This is a far cry from previous simulation packages that require you to formulate differential equations and difference equations in a language or program. Simulink includes a comprehensive block library of sinks, sources, linear and nonlinear components, and connectors. You can also customize and create your own blocks.

After you define a model, you can simulate it, using a choice of integration methods, either from the Simulink menus or by entering commands in MATLAB's command window. The menus are particularly convenient for interactive work, while the command-line approach is very useful for running a batch of simulations. Using scopes and display blocks, you can see the simulation results while the simulation is running. In addition, you can change parameters and immediately see what happens, for "what if"

exploration. The simulation results can be put in the MATLAB workspace for postprocessing and visualization.

The advantage of Simulink is that the user does not have to be concerned about the computer algorithms. However, the user must be able to determine the applicable equations of the system under consideration. Simulink blocks represent mathematical equations. Simulink block diagrams may be written from the equations term by term. The flow is simply:

Problem → *Mathematical Model* → *Block Model* → *Results*

2.5 Simulation with Simulink

Simulink provides a library browser that allows you to select blocks from libraries of standard blocks and a graphical editor that allows you to draw lines connecting the blocks. Any real-world dynamic system can be modeled virtually by selecting and interconnecting the appropriate Simulink blocks.

The time-varying elastance, E(t) for the Left and the Right Ventricles has been realized in the present simulation as shown in the Figure 2.3. Figure 2.4 shows the elastance curves for the Left and Right Ventricles used in this model.

The Figure 2.5 shows the blocks used to realize the Left and Right Ventricles. The basic block diagram is the same for the both the ventricles with only the parameter values being different.

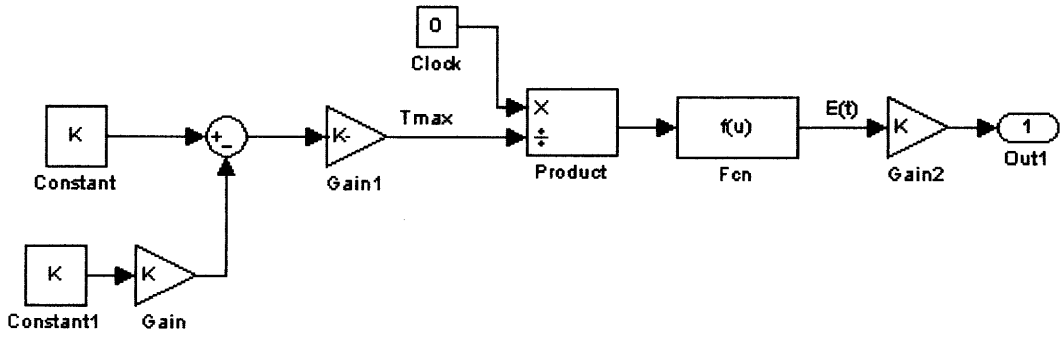

Figure 2.3 Simulink realization for the time-varying elastance for Left and Right Ventricles of the model.

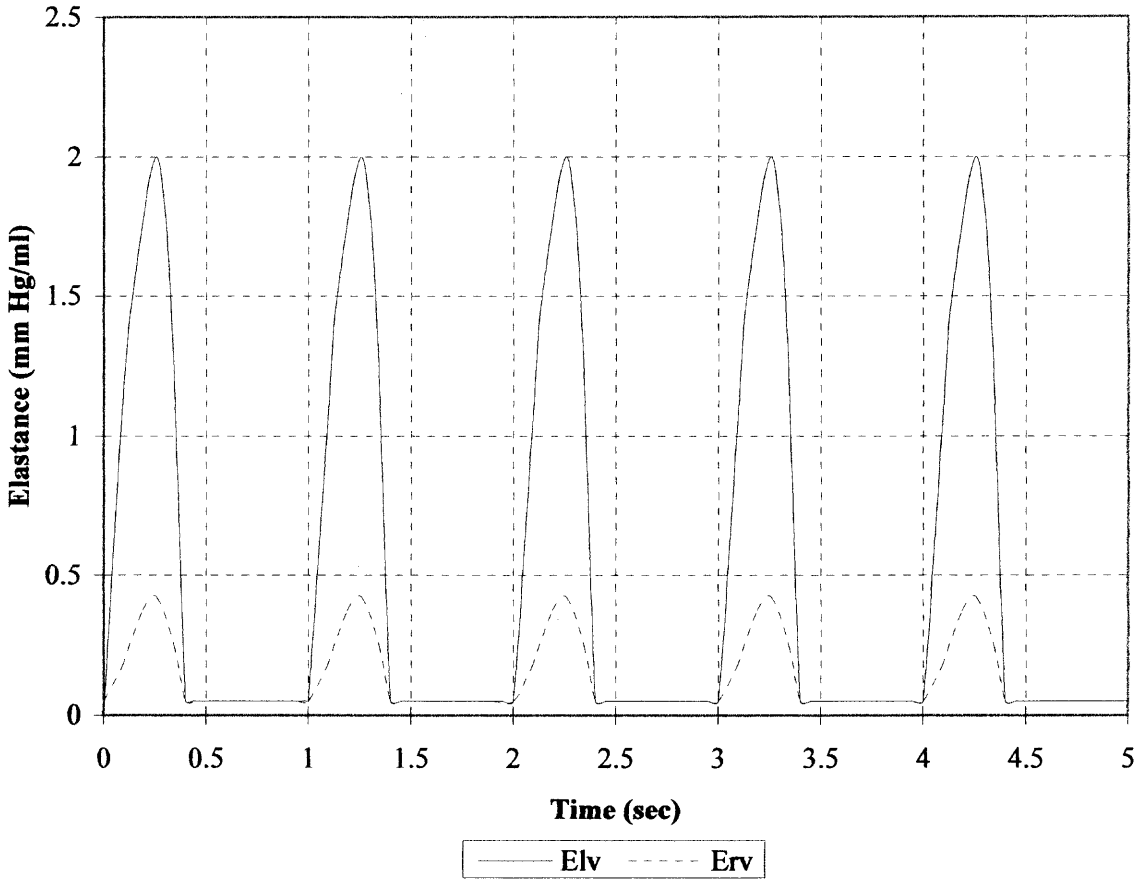

Figure 2.4 Elastance of the Left and Right Ventricles generated by simulation.

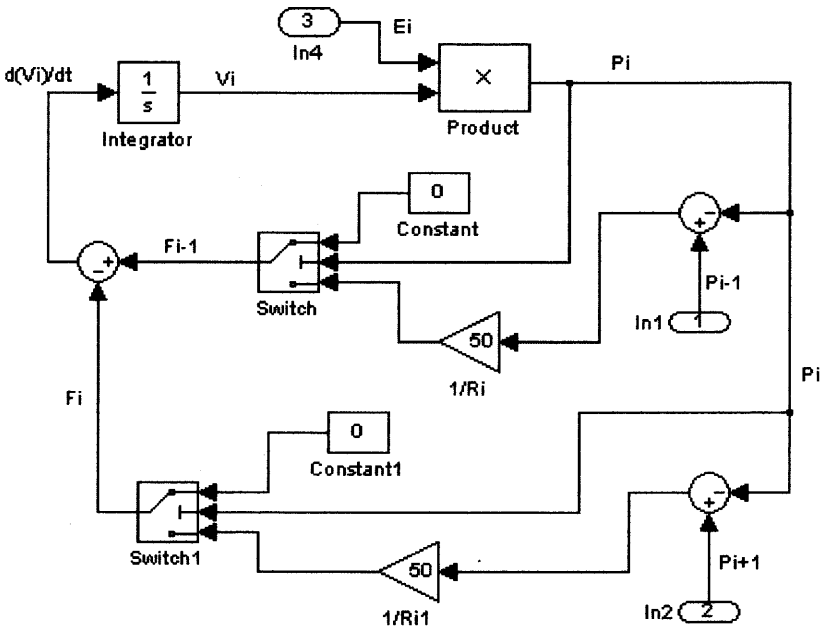

Figure 2.5 Simulink realization for the Left and Right Ventricles compartment of the model.

The Large Arteries III, Systemic Capillaries, Pulmonary Arteries, Pulmonary Capillaries, and Pulmonary Venules compartments in the model have the same layout of blocks (Figure 2.6). The only difference being the parameter values used being specific to the compartments according to the equations stated in the Section 2.3. The compartment *i-1* is downstream of compartment *i* and compartment *i+1* is upstream of compartment *i*.

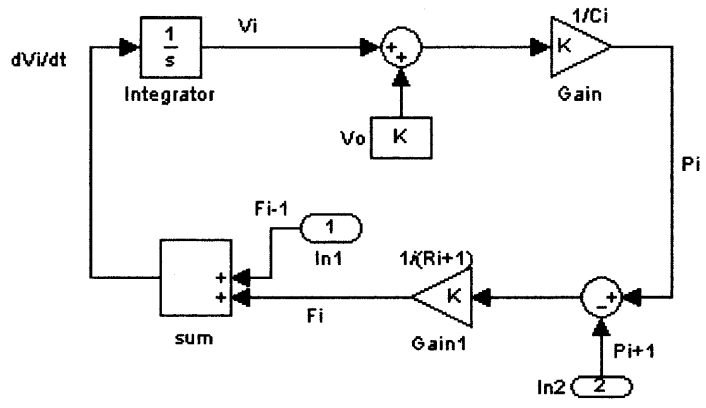

Figure 2.6 Simulink realization for the Large Arteries III, Systemic Capillaries, Pulmonary Arteries, Pulmonary Capillaries and Pulmonary Venules compartments of the model.

The simulink realization of the Aorta is as shown in Figure 2.7. The remaining compartments can be realized as shown in the Appendix A.

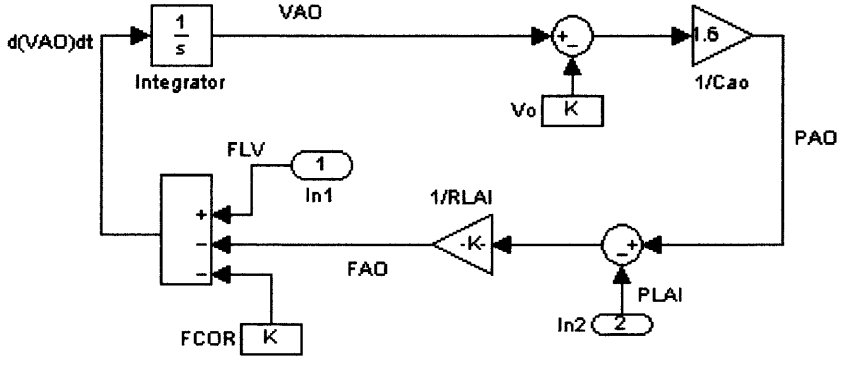

Figure 2.7 Simulink realization for the Aorta compartment of the model.

CHAPTER 3

THE MODEL OF FEEDBACK CONTROL

3.1 A Model for Baroreceptor Reflex Regulation

The baroreceptor mechanism is composed of fast, neurally mediated reflexes that attempt to keep the arterial pressure constant via changes in the output of the sympathetic and parasympathetic nervous systems to the heart and blood vessels. Pressure sensors, the baroreceptors, are located at carotid sinus and aortic arch and relay information about the blood pressure to cardiovascular vasomotor centers in the brain stem. The carotid sinus baroreceptors are responsive to increases or decreases in arterial pressure, whereas the aortic arch baroreceptors are primarily responsive to increases in arterial pressure. In addition, the carotid sinus receptors are more sensitive to pressure than are the aortic arch receptors. Therefore, only the carotid sinus receptors are considered in this model. The carotid arteries are incorporated into the Large Arteries I compartment. Therefore, the blood pressure in the Large Arteries I compartment is taken as the regulated pressure. The mean pressure in the Large Arteries I compartment in a normal human at rest is the set point for baroreceptor reflex. When a sudden change of pressure in the Large Arteries I compartment occurs, the baroreceptor reflex regulates the pressure to the set point by changing ventricular contractility, heart rate, vascular resistance, and capacitance.

In this model, the characterizations of the baroreceptors and their reflex pathways have been included, according to the general structure used by Ottesen [4]. Figure 3.1 illustrates the basic baroreceptor feedback loops.

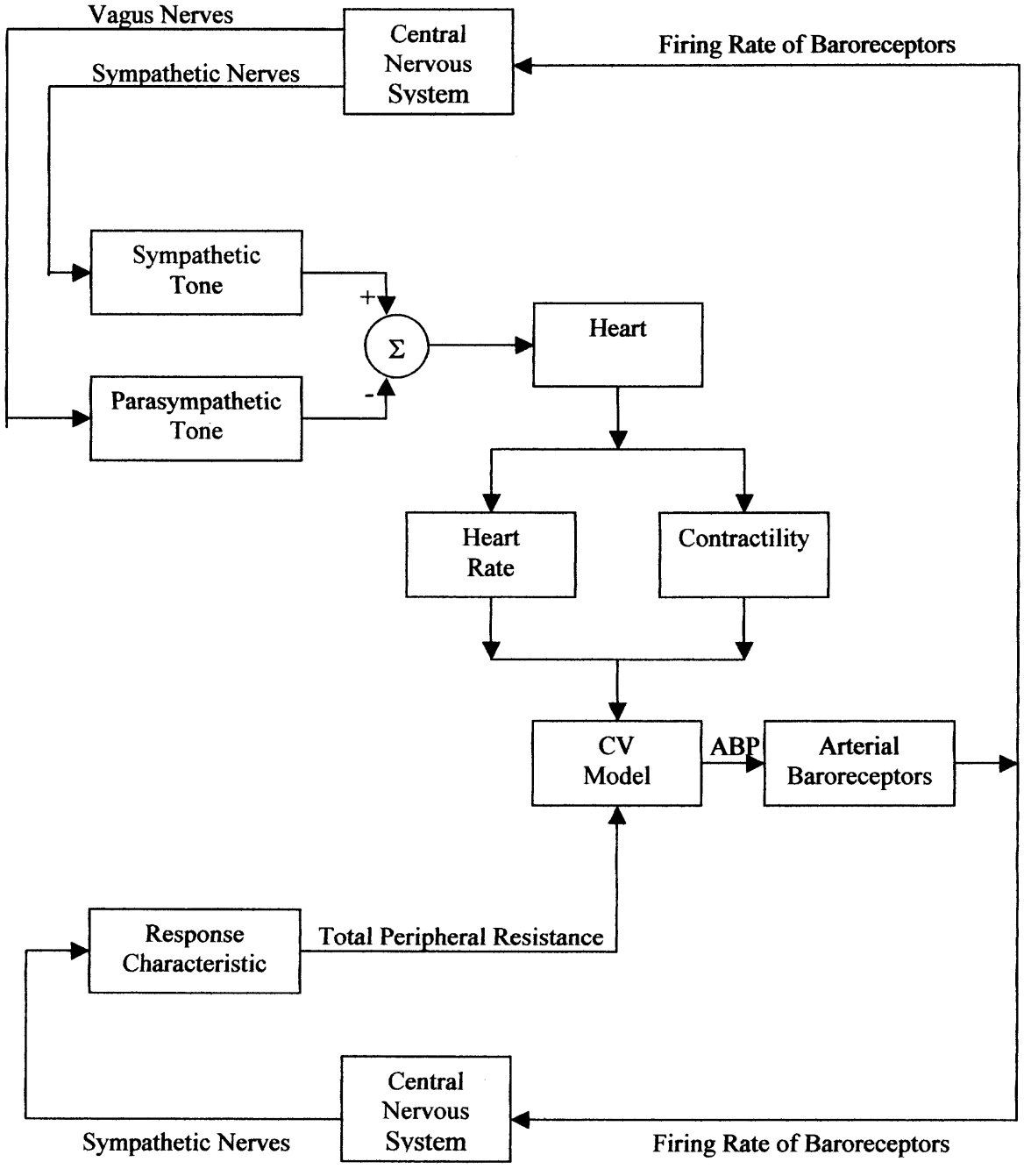

Figure 3.1 Block diagram for baroreceptor regulation mechanism. ABP denotes the arterial blood pressure.

The feedback will be divided into three parts: the affector part where the arterial pressure is the input and the firing rate is the output, the central nervous system where the input is the firing rate and the outputs are the sympathetic and parasympathetic tones (nerve activities), and the effector organs where the tones are inputs and heart rate, contractility, and peripheral resistance are outputs.

3.1.1 The Affector Part

The phrase "the affector part" denotes the part of carotid sinus where the baroreceptors are located together with the baroreceptor nerves, including the axons, as shown in Figure 3.1. When a change in carotid sinus arterial pressure occurs, the cross-sectional area of the sinuses changes, whereby the viscoelastic wall is deformed. The receptors at the nerve endings are located in the lateral wall of the carotid sinus. Hence, a change in pressure causes deformation in the spatial structure, which results in a change in activity of the baroreceptor nerves. This nerve activity is denoted as the firing rate.

Many experiments have been performed to document the baroreceptor response to a change in arterial pressure [4]. The experiments have indicated that the firing rate of the baroreceptor nerves shows several nonlinear characteristics. Firing rate increases with pressure. The response exhibits threshold and saturation. Sufficiently fast decreases in pressure cause firing to drop even below the threshold.

In [4], Ottesen presents and verifies a comprehensive model. Baroreceptors maybe with myelinated axons (MB's) or with unmyelinated axons (UB's). UB's may have two types of discharge: regular and irregular, whereas MB's only discharge regularly. The irregularity is not due simply to a lower frequency of discharge and may

reflect a basic difference in coupling between receptor and vessel wall. This simple model describes the highly nonlinear response in firing rate to changes in carotid sinus arterial pressure. Mathematically it is expressed in terms of nonlinear ordinary differential equations as follows:

$$\begin{aligned}
\dot{\Delta n}_1 &= k_1 \frac{dP_a}{dt}\frac{n(M-n)}{(M/2)^2} - \frac{1}{\tau_1}\Delta n_1 \\
\dot{\Delta n}_2 &= k_2 \frac{dP_a}{dt}\frac{n(M-n)}{(M/2)^2} - \frac{1}{\tau_2}\Delta n_2 \\
\dot{\Delta n}_3 &= k_3 \frac{dP_a}{dt}\frac{n(M-n)}{(M/2)^2} - \frac{1}{\tau_3}\Delta n_3
\end{aligned} \tag{3.1}$$

where n is the firing rate, M the maximal firing rate, dP_a/dt the time derivative of the pressure at carotid sinus, and Δn_1, Δn_2, and Δ_3 denote the derivations from the threshold value N, such that $\Delta n_1 + \Delta n_2 + \Delta n_3 = n - N$. The parameters τ_1, τ_2, and τ_3 are time constants and describe the characteristic adaptation phenomenon measured, for example, by Brown [5]. The parameters k_1, k_2, and k_3 are weighting constants describing the contribution from each receptor type. Typical values are N = 100 mm Hg, M = 150 impulses/sec, τ_1 = 0.5, τ_2 = 5.0, τ_3 = 500 seconds, k_1 = 1.0, k_2 = 2.0, and k_3 = 1.0 Hz/mm Hg. Equivalently, (3.1) may be rewritten in integral form as

$$n = N + \int_{-\infty}^{t}\left(k_1 e^{-((t-s)/\tau_1)} + k_2 e^{-((t-s)/\tau_2)} + k_3 e^{-((t-s)/\tau_3)}\right)\left[\frac{dP}{dt}\frac{n(M-n)}{(M/2)^2}\right]ds \tag{3.2}$$

3.1.2 Central Nervous System

In this section, a model describing how the central nervous system processes the firing rate, n, as an input signal is proposed. The medullary cardiovascular control center is modeled in terms of non-interacting pathways, each characterized by a delay. One vagal

(fast) and one sympathetic (slow) pathway each controls heart rate, whereas two other sympathetic pathways control myocardial contractility and vasomotor tone. The vagal pathway and sympathetic pathways have a 200 ms delay.

3.1.3 The Efferent Parts

In this section, the effector parts of the feedback are treated. The sympathetic and parasympathetic tones are the inputs. The modeling is based on well-established experimental knowledge on the input-output relation in the static situation for each of the effector organs, together with a simple unifying approach describing the dynamics [4].

As the effector organs, the heart and the arterioles are considered (Figure 3.1). The effects are a change in heart rate, H, and peripheral resistance to flow, R. In steady state, heart rate, and peripheral resistance are sigmoidal decreasing functions in firing rate [6-10]. Hence, they are of the form

$$x_{steady}(n) = \frac{x_{\max} - x_{\min}}{1 + \alpha(n/N)^r} + x_{\min} \tag{3.3}$$

with $x = H, R$ and

$$\alpha = \frac{x_{\max} - x_0}{x_0 - x_{\min}},$$

where x_0 is the desired value of x at $n = N$, x_{min} and x_{max} are the minimal and maximal values of x, respectively, n is the time dependent firing rate, given by Equation (3.2), and N is the threshold value described in Section 3.1.1. The range of heart rate used is 40 beats/min to 180 beats/min with the heart rate at the threshold value (N) being 75 beats/min. The minimum and maximum values of resistance correspond to those at an arterial pressure of 40 mm Hg and 180 mm Hg, respectively.

The steady state dependencies are well known from experiments, while the dynamics are only vaguely determined. Hence, the most simple and physiologically justifiable model is chosen to describe the dynamics

$$\frac{dx}{dt} = \frac{1}{\tau_x}\left(x_{steady}(n) - x(t)\right), \tag{3.4}$$

where τ_x is the characteristic time constant describing the transient. Equation (3.4) states that the time-derivative of $x(t)$ is given by the difference between the steady state value, $x_{steady}(n)$, and the actual value, $x(t)$. Notice, that $x_{steady}(n)$ depends on the time-dependent firing rate, and hence is implicitly time-dependent. From [4], it follows that τ_H is two seconds and that τ_R is six seconds, approximately.

The model of the baroreflex-feedback mechanism is given by Equations (3.1) to (3.3), and it requires parameters, all physiologically interpretable and measurable.

CHAPTER 4

METHODS

4.1 Simulation of the Cardiovascular Model

The simulation was implemented using Simulink software program. Simulink is a powerful computer-aided engineering program that provides a complete visual and graphical workspace designing, and plotting models of dynamic systems. Computation was performed with a simulated auto time step size.

The following simulations were implemented:

(1) simulation of the circulation under normal physiological condition at rest to provide a baseline for comparison under other conditions.

(2) to investigate the effects of baroreceptor reflexes, the regulatory effects on sudden changes in blood pressure caused by sudden changes in left ventricular contractility and in peripheral resistance were simulated.

Using the parameters given in Table 2.1, the waves of pressures and volumes of each compartment in a normal human at rest were obtained in the first series of simulations. Figure 4.1 shows the pressure in the Left Ventricle. Figure 4.2 shows the volume waveform of the Left Ventricle generated by simulation. Stroke volume is 74.7 ml. Cardiac output is 5602.5 ml/min. The maximum and minimum values of pressure and volume are given in the Table 4.1. The end-systolic pressure approximates the maximum pressure. The minimum pressure used is the end-diastolic pressure. The maximum volume is the end-diastolic volume and the minimum volume is the end-systolic volume.

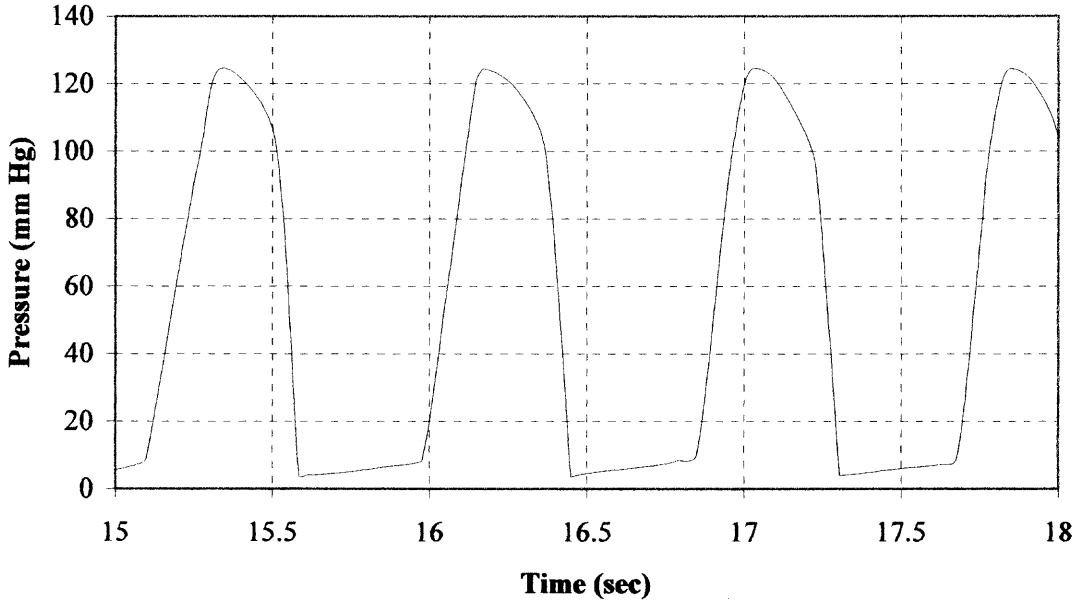

Figure 4.1 Blood pressure in the Left Ventricle generated by the simulation.

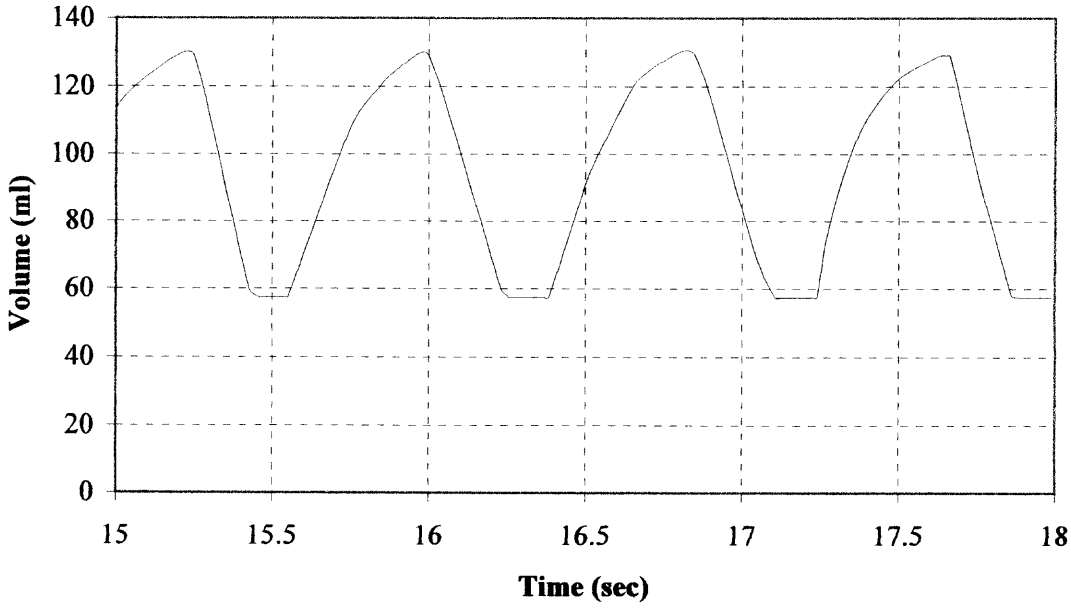

Figure 4.2 Blood volume of the Left Ventricle generated by the simulation.

The pressure and volume waveforms of the remaining compartments generated by simulation are shown in Appendix C.

Table 4.1 Range of Blood Pressure and Volume Generated by Simulation.

(Normal Human at Rest)

	Pressure (mm Hg)	**Volume (ml)**
Left Ventricle	124.5 – 4.4	129.1 – 54.4
Aorta	121.5 – 74.22	135.9 – 106.4
Large Arteries I	96.8 – 69.3	127.5 –106.8
Large Arteries II	77.9 – 65.6	147.9 – 135.2
Large Arteries III	67.86 – 60.64	143.4 – 135.5
Arterioles	28.69 – 27.65	104.2 – 102.5
Systemic Capillaries	10.33 – 10.32	323.7 – 323.6
Venules	7 – 6.96	459.6 – 458.4
Large Veins	6.77 – 6.71	2648 – 2644
Vena Cava	5.4 – 3.28	346.5 – 312.9
Right Ventricle	26 – 3.61	125.3 – 51.85
Pulmonary Arteries	14 – 6.75	170.5 – 133
Pulmonary Capillaries	10.6 – 6.7	123.8 – 105.6
Pulmonary Venules	8.86 – 5.6	237 - 207

4.2 Demonstration of Physiology

Changes in the heart rate have been used in many papers to analyze the relationships of the heart with the rest of the circulatory system (i.e., with the preload and afterload). Various authors observed that heart pacing causes controversial effects on cardiac output: while in some instances cardiac output increases with heart rate, in others it remains unchanged or may even decrease [21].

The Figure 4.3 confirm the existence of a different effect of heart rate changes on cardiac output, depending on ventricular filling and stroke volume. If the heart rate is increased from 60-80 beats/min (which corresponds to normality in humans), cardiac output will increase, but this increase is far less than proportional to the increase in rate for two reasons, (1) with the increase in cardiac output, blood is removed from the venous vessels, filling pressure (preload) falls, and stroke volume decreases, and (2) the increased cardiac output will increase the arterial pressure (afterload), and this will decrease the stroke volume. If the peripheral resistance remains constant, arterial pressure, like cardiac output, will rise proportionally less than heart rate. If heart rate were to increase in this fashion in an unstressed individual with normal reflex responses, reflex effects on peripheral vessels and on cardiac contractility will also act to decrease arterial pressure. But even without reflexes, cardiac output and arterial pressure will change far less than heart rate. By contrast, when heart rate is above 90 beats/min, its changes have almost no effect on cardiac output. If the heart rate becomes so high (>130 mm Hg) that the time for rapid ventricular filling is decreased, cardiac output will plateau and then may even decrease with further increases in rate. This physiology is well exhibited by the present cardiovascular model as shown in the Figure 4.3.

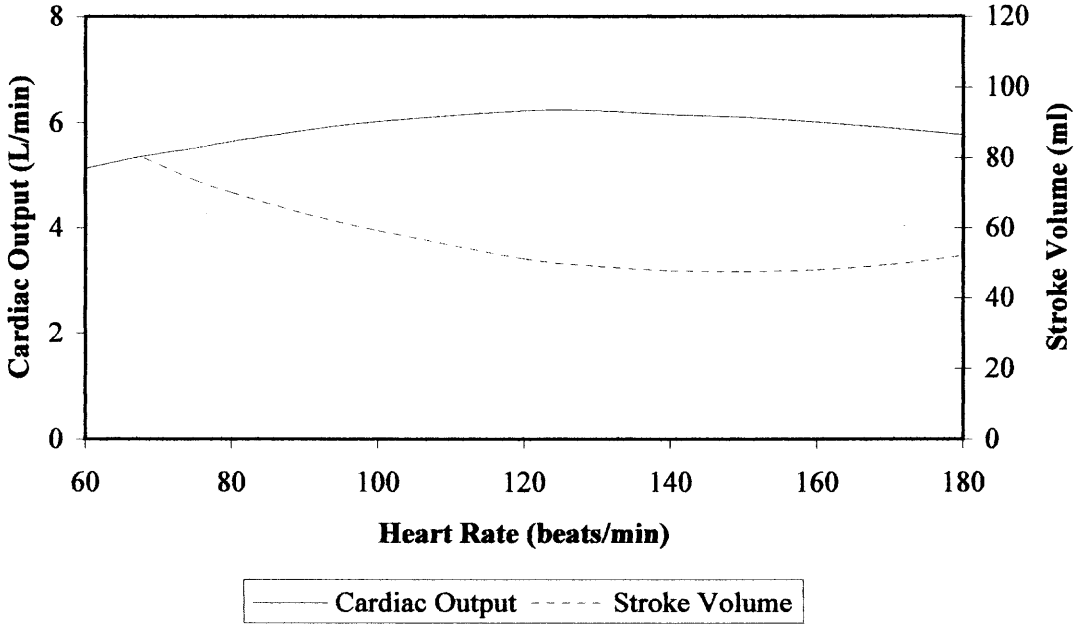

Figure 4.3 Effects of changing heart rate over a wide range of cardiac output and stroke volume.

The function of the Left Ventricle can be observed over an entire cardiac cycle (diastole plus systole). The ventricular pressure-volume loop describes one cycle of ventricular contraction, ejection, relaxation and refilling. The Figure 4.4 shows the pressure-volume loop of the Left Ventricle as generated by the cardiovascular model.

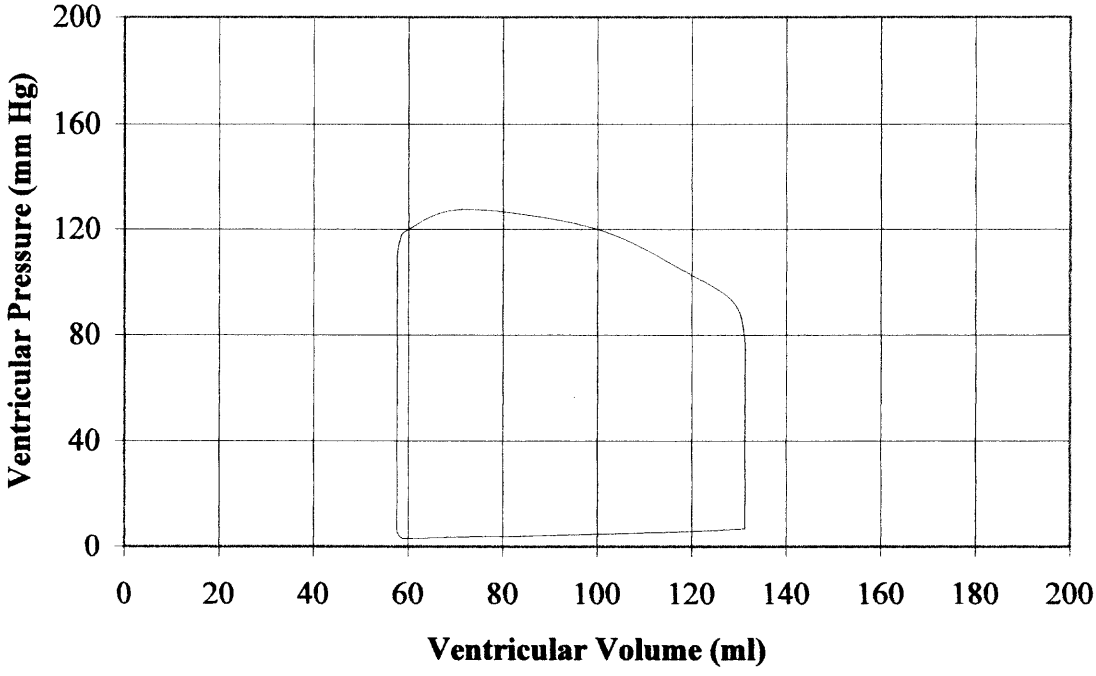

Figure 4.4 Pressure-volume loop of the Left Ventricle.

The Frank-Starling law of the heart, or the Frank-Starling relationship, states that the volume of blood ejected by the ventricle depends on the volume present in the ventricle at the end of diastole. The volume present at the end of diastole, in turn, depends on the volume returned to the heart, or the venous return. Therefore, stroke volume and cardiac output correlates directly with end-diastole volume, which correlates with venous return. The Frank-Starling relationship governs normal ventricular function and ensures that the volume the heart ejects in systole equals the volume it receives in venous return. This relationship is illustrated in Figure 4.5. Stroke volume is plotted as a function of ventricular end-diastolic volume. There is a curvilinear relationship between stroke volume and ventricular end-diastolic volume. As venous return increases, end-diastolic volume increases and, because of the length-tension relationship, stroke volume increases accordingly. In the physiologic range, the relationship between stroke volume and end-diastolic volume is nearly linear. Only when end-diastolic volume becomes very high does the curve start to bend.

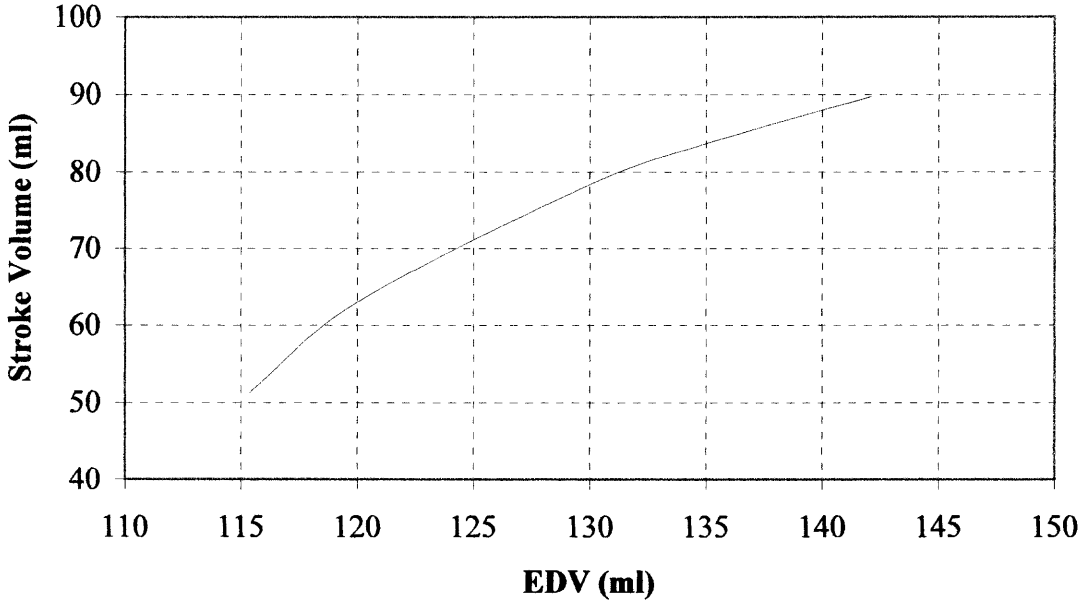

Figure 4.5 Stroke volume plotted as a function of end-diastolic volume.

CHAPTER 5

RESULTS

To investigate the effects of baroreceptor reflexes, the regulatory effects on sudden changes in blood pressure caused by sudden changes in left ventricular contractility and in peripheral resistance were simulated. Four simulations were performed using the following conditions:

(a) left ventricular contractility was decreased by 50%.

(b) left ventricular contractility was decreased by 50%. After 60 seconds, it was set to its normal value.

(c) peripheral resistance was increased 25%.

(d) peripheral resistance was increased 25%. After 60 seconds, it was set to its normal value.

Figures 5.1 and 5.2 show the result of a simulation where the contractility of the Left Ventricle was decreased by 50%. As a consequence, a drop of arterial pressure from the actual heartbeat to the next follows. The baroreflex feedback mechanism reacts by raising the heart rate and the peripheral resistance. The arterial pressure stabilizes at a new "steady state" level. The heart rate shows some overshooting before it approaches the new "steady state" level.

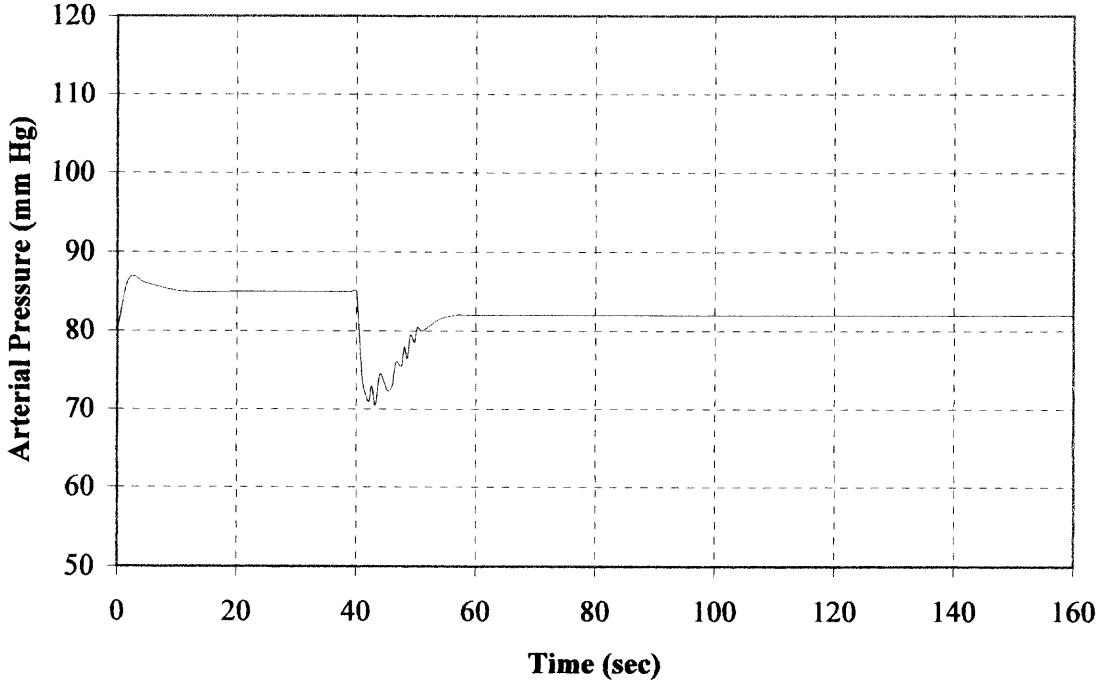

Figure 5.1 The time course in arterial pressure due to a drop in contractility.

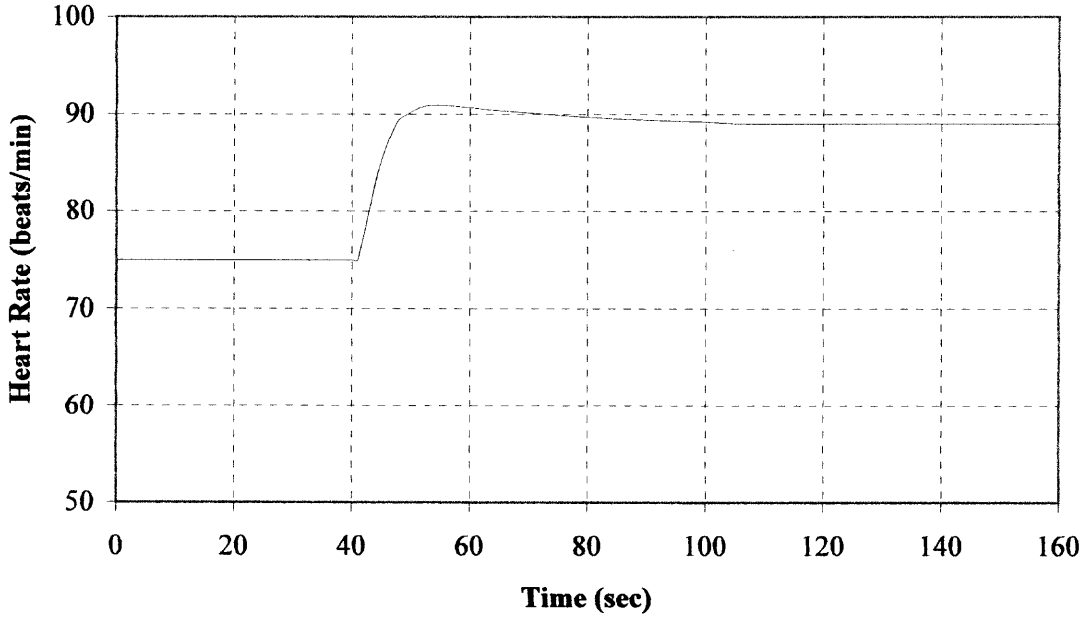

Figure 5.2 The time course of heart rate due to a drop in contractility.

Figures 5.3 to 5.5 show the effects of baroreceptor reflex on the sudden decrease in blood pressure caused by the sudden decrease in left ventricular contractility at 40 sec after the onset of simulation. After the regulation of the baroreceptors, the arterial pressure was brought back to the set point. The baroreflex feedback sets in to raise the heart rate and the peripheral resistance. After 100 sec from the onset of simulation, left ventricular contractility was increased to its normal value. This resulted in a sudden increase in blood pressure. After the regulatory mechanism, the arterial pressure was back to the set point; heart rate and total peripheral resistance were decreased to their normal value.

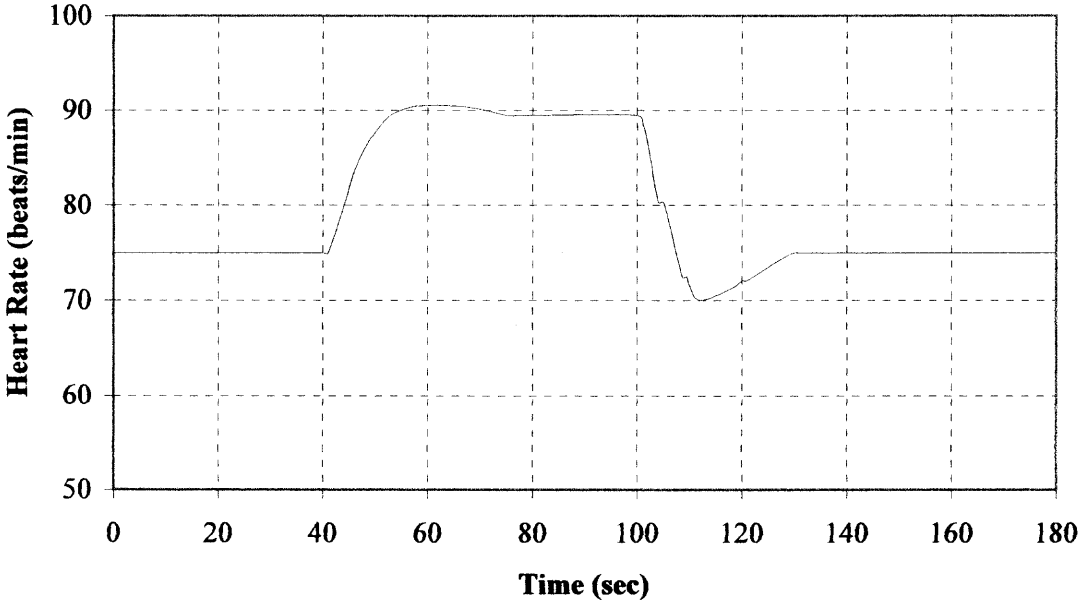

Figure 5.3 The effect of baroreceptor reflex on a sudden decrease of blood pressure caused by sudden decrease of left ventricular contractility, (a) heart rate.

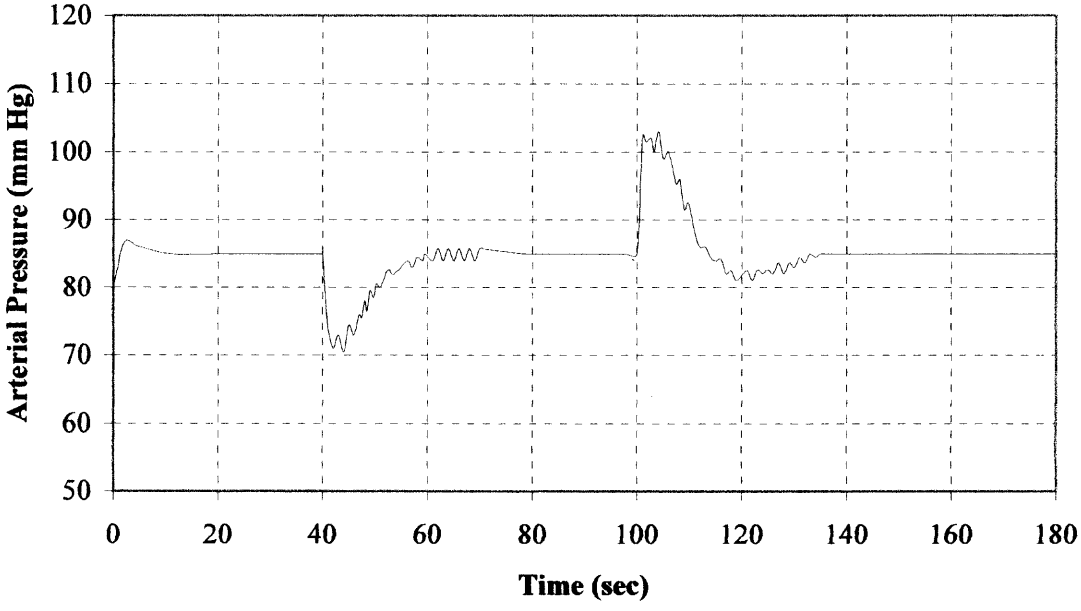

Figure 5.4 The effect of baroreceptor reflex on a sudden decrease of blood pressure caused by sudden decrease of left ventricular contractility, (b) pressure.

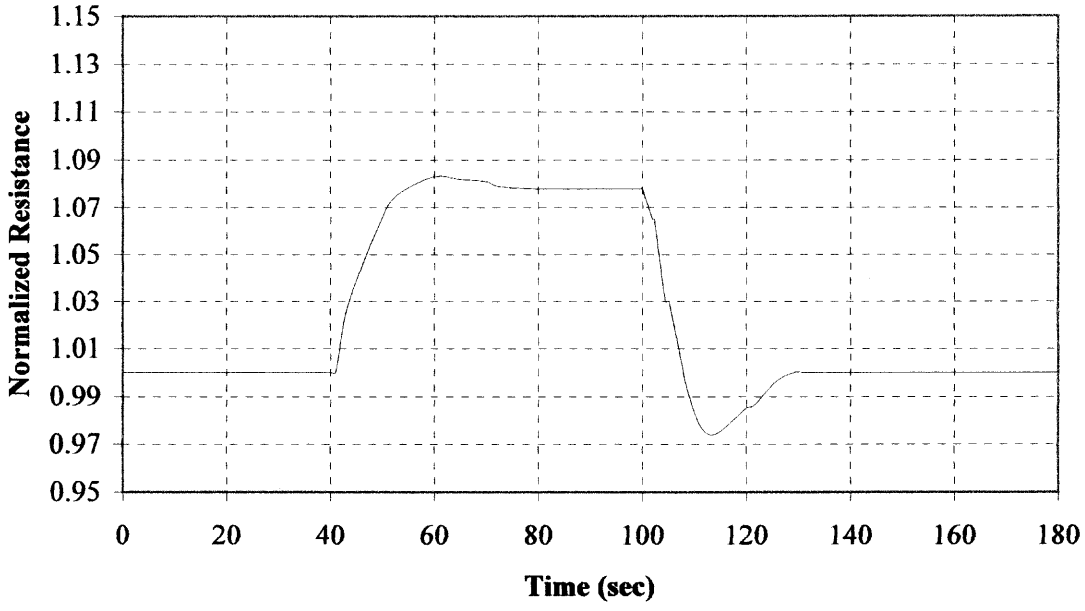

Figure 5.5 The effects of baroreceptor reflex on a sudden decrease of blood pressure caused by the sudden decrease of left ventricular contractility, (c) (value of total peripheral resistance) / (normal value of total peripheral resistance).

Figures 5.6 and 5.7 show the results of simulation where the peripheral resistance is increased by 25%. As a consequence, a rise in arterial pressure over a few seconds follows. The feedback regulation of the baroreceptors reacts by lowering the heart rate. Hence, the pressure and heart rate show a little overshooting before they approach the new "steady state" level. This behavior is in harmony with clinical observations, where the peripheral resistance is raised either by drugs or by mechanical clamping of vessels.

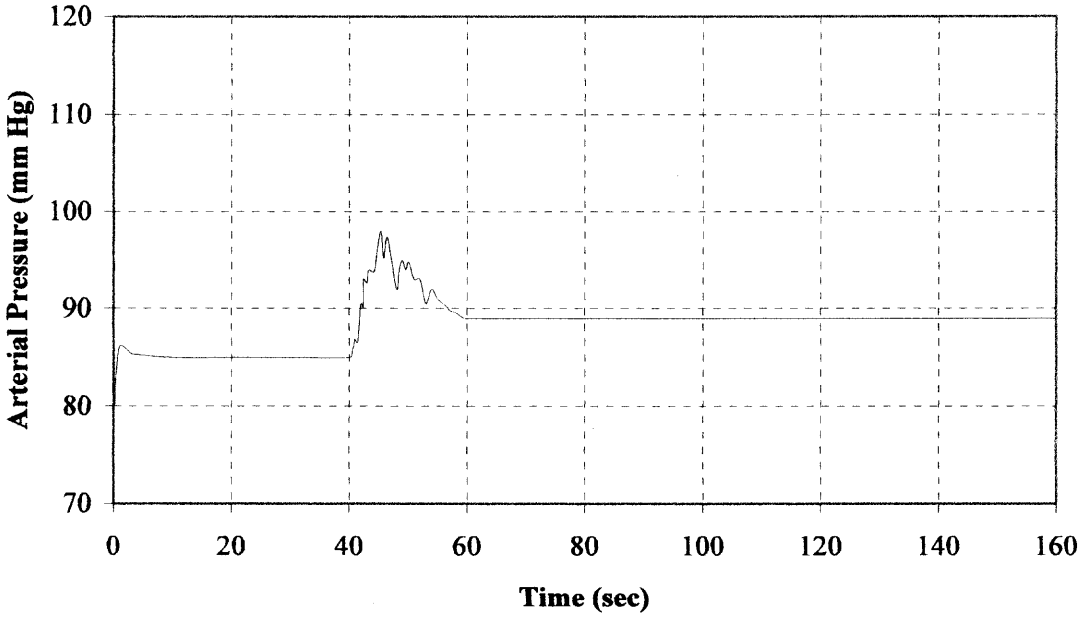

Figure 5.6 The time course in arterial pressure due to an increase in peripheral resistance.

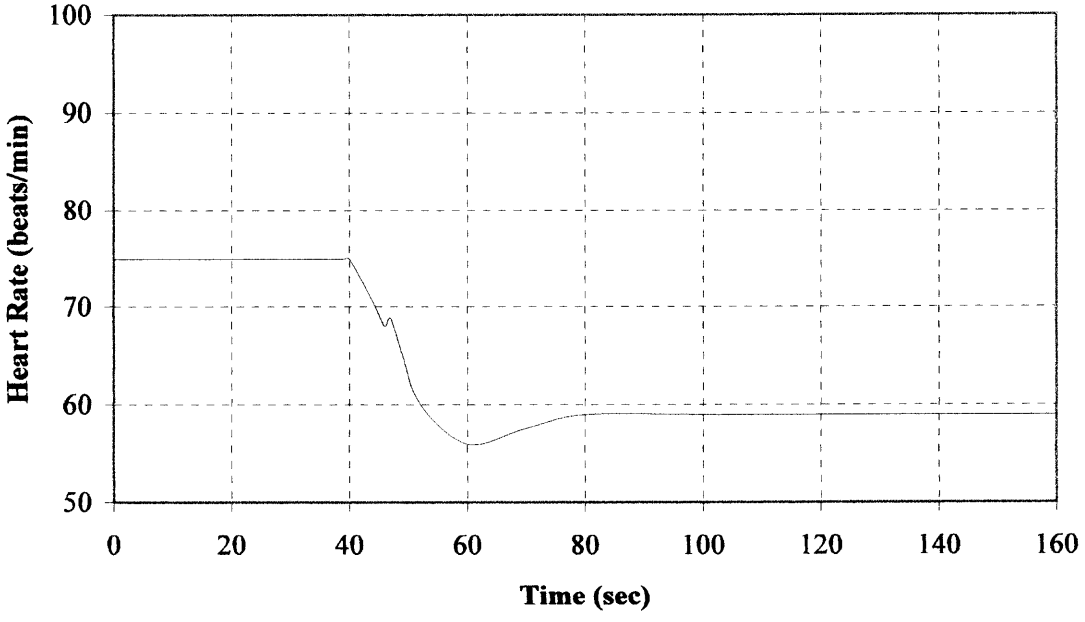

Figure 5.7 The time course in heart rate due to an increase in peripheral resistance.

Figures 5.8 and 5.9 show the effects of baroreceptor reflex on the sudden increase in blood pressure caused by the sudden increase in total peripheral resistance by 25 % of the normal value at 40 sec after the onset of simulation. After the regulation of baroreceptor reflex, the arterial pressure was back to set point. As a consequence, a rise in arterial pressure over the next few seconds follows. The baroreflex-feedback mechanism reacts by lowering the heart rate and the increased peripheral resistance, which cause the arterial pressure to be lowered. At 100 sec after onset of simulation, total peripheral resistance decreased by 25% of its normal value. This resulted in a sudden decrease in blood pressure. Heart rate and total peripheral resistance also rise back to their normal value. After the regulatory mechanism of the baroreceptors, the arterial pressure was brought back to normal.

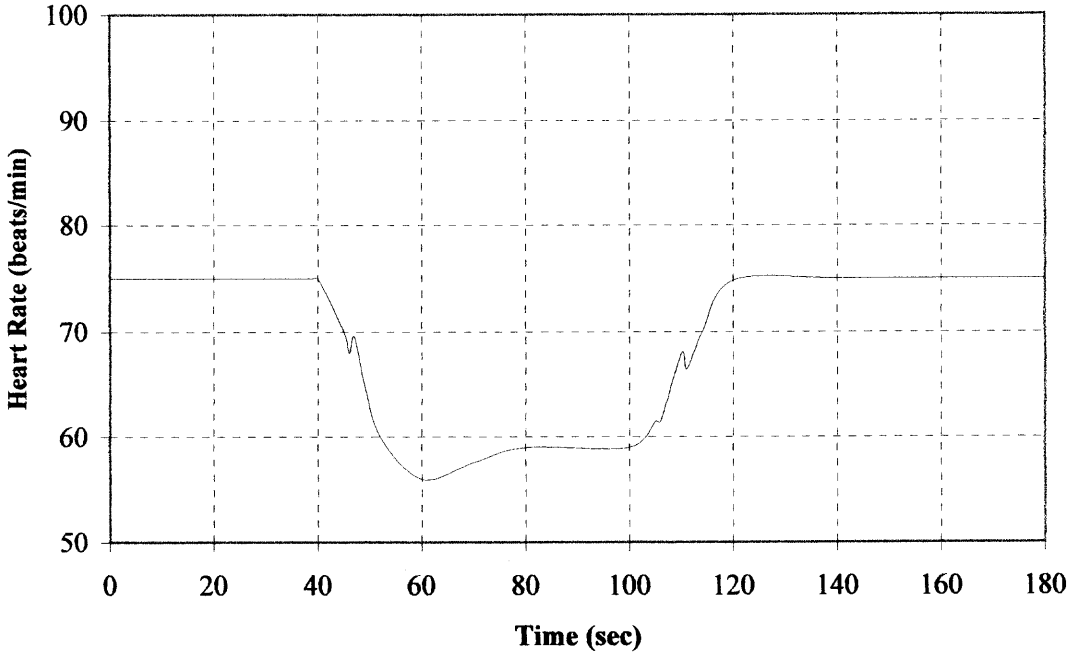

Figure 5.8 The effects of baroreceptor reflex on a sudden increase of blood pressure caused by the sudden increase of peripheral resistance, (a) heart rate.

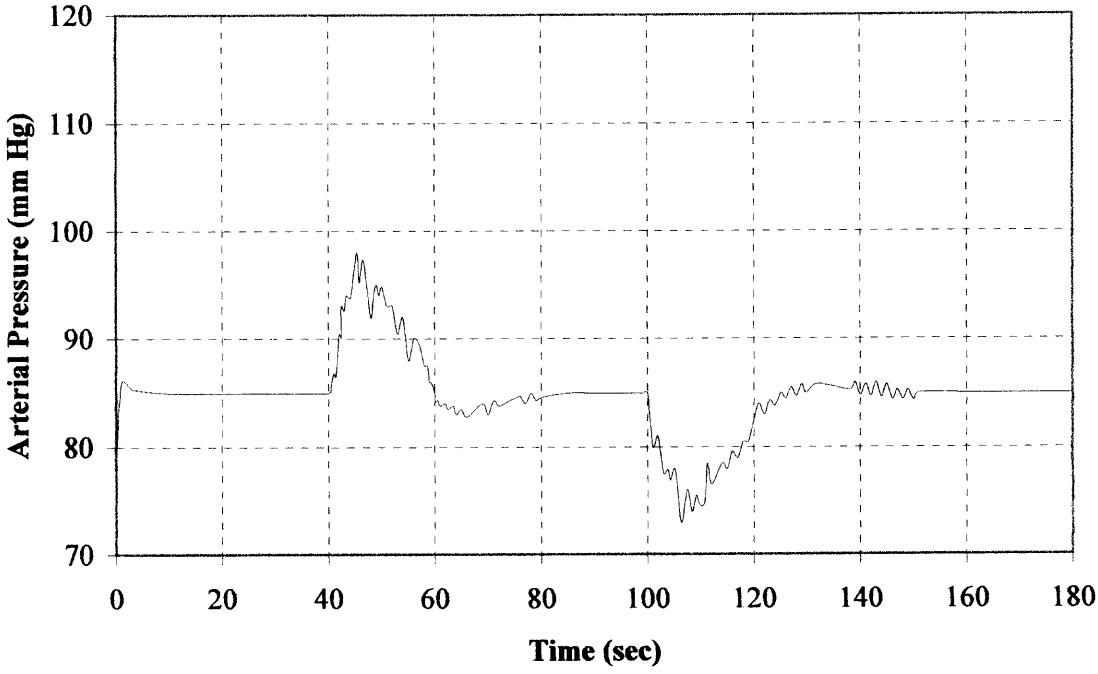

Figure 5.9 The effects of baroreceptor reflex on a sudden increase of blood pressure caused by the sudden increase of peripheral resistance, (b) pressure.

CHAPTER 6

DISCUSSIONS AND SCOPE

6.1 Discussion

A general procedure for mathematical modeling should follow a logical progression that optimizes the model for the particular application. The generation of an accurate model involves an iterative process of modifying existing model parameters and the reinterpretation of experimental data. Once the parameters are well defined and the equations are expressed, the model should be ready to be tested.

The described model combines accepted models of the cardiovascular system and the baroreflex regulation. The model represents an important step in understanding the role of the baroreceptor reflex regulation mechanism. An important aspect is the distinction between the different functional parts of the baroreflex, i.e., the afferent pathway, the central nervous processing system, and the peripheral effectors. This distinction may enable improved understanding of the possible role of each part in baroregulation, and of the consequences of their pathological changes. Predictions of the model agree with experimental and clinical observations and provide useful insights into the role of contributing variables that are difficult to manipulate in real life. Given the normal values for cardiovascular parameters, the model predicts acceptable values for blood volumes and pressure. The left ventricular pressure and volume curves are characteristic in appearance.

By far the best known of the nervous mechanisms for arterial pressure control is the *baroreceptor reflex*. The baroreceptors respond extremely rapidly to changes in

arterial pressure; in fact, the rate of impulse firing increases in the fraction of a second during each systole and decreases again during diastole. The net effect of the baroreceptor signals are: (1) *vasodilation* of the veins and arterioles throughout the peripheral circulatory system, and (2) *decreased heart rate* and *strength of contraction.* Therefore, the excitation of the baroreceptors by pressure in the arteries reflexly causes the arterial pressure to decrease because of both a decrease in peripheral resistance and a decrease in cardiac output. Conversely, low pressure has opposite effects, reflexly causing the pressure to rise back to normal.

Model Limitations

The following major simplifications and assumptions were used in the construction of the present mathematical model.

1. A lumped parameter model was used in the present study. The compartmental approach assumes that the cardiovascular system can be divided into a number of units. The behavior of each unit is represented by pressure for that unit and the flow and resistance between adjacent units. Moreover, this particular model considers only the cardiovascular system and does not incorporate systems like renal, pulmonary etc.
2. Changes in blood viscosity affect regional vascular resistances. The model does not consider this relationship.
3. In the present model, the compliance of the arterial compartment is constant throughout the cardiac cycle. However, the compliance of arteries, especially in the Aorta, is a time-varying parameter.

Despite these limitations, the model predictions agree with the experimental and clinical observations and provide useful insights into the role of the baroreceptors in the regulation of the arterial pressure. Simulation allows for a better understanding of the regulatory mechanism by changing various parameters.

6.2 Future Work

6.2.1 The Overall Concept of a Model for Autoregulation

If tissue is to receive the oxygen and nutrients required for metabolism and to have waste products removed, the flow of blood through the tissue must be adequate. This flow through each organ is regulated in part by local and in part by central arrangements, which change the vascular resistance to blood flow. For this mechanism to be effective, the systemic arterial pressure must be held reasonably constant by homeostatic mechanisms. With a constant blood pressure, the flow of blood through an organ or tissue is inversely related to its vascular resistance. To maintain constant systemic blood pressure as the flow through a tissue increases, either the cardiac output must be increased or the flow through some other region must be reduced.

One of the mechanisms, which are responsible for autoregulation of blood flow, is that the rate of oxygen extraction from the blood equals the rate of oxygen consumption by tissue. This equilibrium is maintained by active changes in vascular resistance affecting the blood flow and by changes in the arteriovenous oxygen content difference $(O_{2a} - O_{2v})$. The oxygen supply to tissue (ml O_2/sec) is calculated as follows:

$$M_s = F_t(O_{2a} - O_{2v}) \tag{6.1}$$

where M_s is the rate of oxygen supply to tissue. F_t is the average blood flow in tissue. O_{2a} and O_{2v} are the oxygen concentrations in the arteries and veins, respectively. F_t is defined by Equation (6.2).

$$F_t = (P_u - P_d)/R_t \tag{6.2}$$

where P_u and P_d are the blood pressures upstream and downstream of the tissue or organ being autoregulated. R_t is the hemodynamic resistance between the upstream and downstream points. From Equations (6.1) and (6.2), the resistance between the two points can be calculated as follows:

$$R_t = [(P_u - P_d)(O_{2a} - O_{2v})] / M_s \tag{6.3}$$

M_c is defined as the rate of oxygen consumption by the tissue or organ. The oxygen consumption rate must be equal to the rate of oxygen supply to satisfy the law of mass conservation. Therefore, the rate of oxygen supply, M_s can be substituted with the rate of oxygen consumption; M_c and Equation (6.3) can be changed as follows:

$$R_t = [(P_u - P_d)(O_{2a} - O_{2v})] / M_c \tag{6.4}$$

In the present model, the complex relationship between the coronary resistance and arteriovenous coronary oxygen difference $(O_{2a} - O_{2v})$ is not considered and the coronary oxygen difference is assumed to be constant throughout the active range of autoregulation (*0.14 ml O_2/sec*). From Equation (6.4), it is evident that the resistance of the tissue or organ varies with the pressure and the rate of oxygen consumption. The direction of the change in resistance is determined experimentally.

6.2.2 A Model for Autoregulation in the Coronary Artery

In many pathological situations, such as obstructive coronary artery disease, the oxygen requirements of the myocardial tissue may exceed the capacity of coronary blood flow to deliver oxygen to the heart muscle. It is important, therefore, to understand what factors determine the myocardial oxygen consumption rate because reduction of oxygen demand may be of significant clinical benefit to the patient.

The energy expended during the isovolumetric contraction phase of the cardiac cycle accounts for the largest portion (~ 50 percent) of the total myocardial oxygen consumption despite the fact that the heart does no external work during this period. The energy needed for isovolumetric contraction depends heavily on the intraventricular pressure that must develop during this time, i.e., on the cardiac afterload. *Cardiac afterload* then is a major determinant of myocardial oxygen consumption. Reductions in cardiac afterload can produce clinically significant reductions in myocardial energy requirements and therefore, myocardial oxygen consumption. Actually, energy utilization during isovolumetric contraction is more directly related to isometric *wall tension* development than to its intraventricular pressure development.

It is during the ejection phase of the cardiac cycle that the heart actually performs external work and the energy the heart expends during ejection depends on how much *external work* it is doing. Changes in *myocardial contractility* can have important consequences on the oxygen requirement for basal metabolism, isovolumic wall tension generation, and external work.

Heart rate is also one of the more important determinants of myocardial oxygen consumption. It has been found that it is more efficient (less oxygen is required) to achieve a given cardiac output with low heart rate and high stroke volume than with high heart rate and low stroke volume.

There are many indexes such as tension-time index (*TTI*), tension-time or force-time integral (*FTI*), rate-pressure product (*RPP*), pressure-work index (*PWI*) and systolic pressure-volume area (*PVA*) which have been developed as predictors of myocardial oxygen consumption. In Takaoka's study [18], they assessed the relationship between these indexes and myocardial oxygen consumption per beat. Their results demonstrated that *PVA* is the best predictor of myocardial oxygen consumption among these indexes.

PVA was defined by Suga [19] as the area in the pressure-volume plane that is enclosed by the diastolic curve, the systolic pressure-volume curve, and the tangent line-E_{max}. *PVA* is considered as the driving energy of a ventricle per heartbeat. *PVA* can be divided into external or pumping work (W_E) that is related to ejection contraction, and mechanical potential energy (W_P) that corresponds to isovolumic contraction. W_E is calculated by integrating the ventricular pressure in systole and diastole with respect to the volume.

According to Suga's study, the oxygen consumption rate of 100g left ventricle (M_{cor}) per beat is calculated as follows:

$$M_{cor} = A \times PVA + B \times E_{\max} + C \tag{6.5}$$

where *PVA* is calculated as the pressure-volume area per 100g of left ventricle and the coefficients A, B, and C are as follows:

$A = 1.8 \times 10^{-5}\ ml O_2 / (mmHg\ ml)$

$B = 2.4 \times 10^{-3}\ (ml O_2\ ml) / (beat\ mmHg\ ml\ 100g)$

$C = 0.014\ ml O_2 / (beat\ 100g)$

The upstream pressure of the coronary artery is the pressure in the aorta (PAO). The downstream pressure of the coronary artery is the pressure in the coronary sinuses. The coronary sinus pressure can be approximated as the pressure in vena cava (P_{VC}). In addition to driving blood through the coronary vessels, the heart also influences its blood supply by squeezing effect of the contracting myocardium on the blood vessels. This force is so great during early ventricular systole that blood flow in a large coronary artery supplying the left ventricle is briefly reversed. The pressure caused by squeezing of the heart muscle is calculated from ventricular pressure and is equal to $0.75P_{lv}$ [3]. Therefore, the resistance of the coronary arteries is calculated as follows:

$$R = \left[\left(PAO - 0.75P_{lv} - P_{vc}\right) \times \left(O_{2a} - O_{2v}\right)\right] / M_{cor} \tag{6.6}$$

The arteriovenous oxygen difference $(O_{2a}\text{-}O_{2v})$ across the coronary arteries is assumed to be constant throughout the active range of autoregulation. $(O_{2a}\text{-}O_{2v})$ can be calculated as a product of $O_{2a} = 0.194\ (ml\ O_2/ml\ blood)$ and the normal oxygen uptake ratio which is 0.647.

6.2.3 Circulation in Specific Organs

The volume of blood ejected from the left ventricle during systole is distributed to the various tissues, which are arranged in parallel. Consequently, the major determinant of cardiac output distribution is the relative vascular resistance that exists among the various vascular beds.

Active regulation is seen in an organ, which tends to adjust the caliber of its resistance vessels. The organ in this manner holds its blood flow relatively constant in the face of changes in perfusion pressure. The following circulatory systems manifest this type of behavior: cerebral, kidney, coronary, hepatic artery, intestine, and muscle. The rate of metabolism in these organs is assumed to be constant at rest, while arterial and venous oxygen concentrations of these organs are also constant. From Equation (6.1), it is evident that blood flow (F) should be constant to maintain a constant metabolic rate. Therefore, the resistance of organs changes to maintain a constant flow when perfusion pressure changes. The resistances of these organs are calculated as follows:

$$K = F(T) \,/\, F_0 \tag{6.7}$$

$$R(T+1) = K \times R(T) \tag{6.8}$$

where K is a control factor. F_0 is a predetermined set point for flow (i.e. the flow in a certain organ or tissue is maintained at F_0 by autoregulation). $F(T)$ is the average preregulated flow during a cardiac period T. $R(T+1)$ and $R(T)$ are the regulated and preregulated resistance. During a simulation, resistance is adjusted by beat-to-beat autoregulation. Since the autoregulation is active only over a limited range of perfusion pressure, the resistance has upper and lower limits, which can be calculated using the Equation (2.1), i.e. the upper and lower resistances can be calculated by dividing the upper and lower perfusion pressure by the predetermined set point for flow.

APPENDIX A

BLOCKS USED IN SIMULINK

This section documents the exact syntax of the Simulink blocks. Many blocks have "parameters". These are the constant coefficients for the functions. Undefined parameters are assigned default values by Simulink.

Action

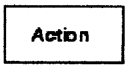

The Action Block implements the Action subsystems used by If and Switch control flow statements in Simulink. There are no data inputs or outputs for Action Port block.

Action Subsytem

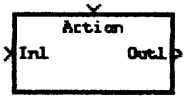

This block is a Subsystem block that is preconfigured to serve as a starting point for creating a subsystem whose execution is triggered by an If or Switch Case block.

Clock

This block displays and provides the simulation time. The Clock block outputs the current simulation time at each simulation step. This block is helpful for other blocks that need the simulation time. The Decimation parameter value is the increment at which the

clock gets updated; it can be any positive number. For example, if the decimation is 1000 then for a fixed integration step of 1 millisecond, the clock will update at 1 second, 2 seconds, and so on.

Constant

This block generates a constant value. The Constant block generates a specified real or complex value independent of time. The block generates one output whose numeric type (real or complex) and data type are the same as that of the block's Constant value parameter.

Fcn

The Fcn block applies the specified C language style expression to its input. The expression must be mathematically well formed.

Gain

The Gain block generates its output by multiplying its input by a specified gain factor. You can enter the gain as a numeric value, or as a variable or expression in the Gain parameter field.

If

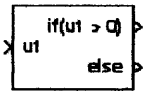

The If block, along with Action subsystems containing Action port blocks, implements standard C-like if-else logic. The If block accepts number of inputs that appear as data input ports labeled with a 'u' character followed by a number 1,2,...,n where n equals the number of inputs that you specify.

Integrator

The Integrator block integrates its input. The output is simply its state, the integral. The Integrator allows you to: 1) define initial conditions on the block dialog box or as input to the block, 2) output the block state, 3) define upper and lower limits on the integral, and 4) reset the state depending on an additional reset input.

Product

The Product block outputs the element-wise or matrix product of its inputs, depending on the values of the Multiplication and Number of inputs parameters. The Product block accepts real- or complex-valued signals of any data type for element-wise multiplication. All input signals must be of the same data type. The output signal data type is the same as

the input's. The inputs must be real or complex signals of type single or double for matrix multiplication.

Sum

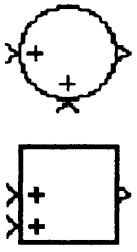

The Sum block adds scalar, vector, or matrix inputs or the elements of a single vector input. It accepts real- or complex-valued signals of any data type.

Switch

The Switch block propagates one of two inputs to its output depending on the value of a third input, called the control input. If the signal on the control (second) input is greater than or equal to the Threshold parameter, the block propagates the first input; otherwise, it propagates the third input. A Switch block accepts real- or complex-valued signals of any data type as switched inputs (inputs 1 and 3). Both switched inputs must be of the same type. The block output signal has the data type of the selected input. The type of the threshold input must be boolean or double.

APPENDIX B

SIMULINK REALIZATION OF THE COMPARTMENTAL MODEL

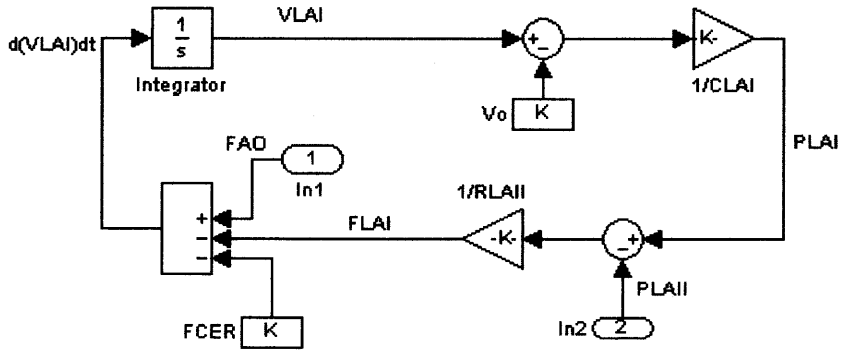

Figure B.1 Simulink realization for the Large Arteries I compartment of the model.

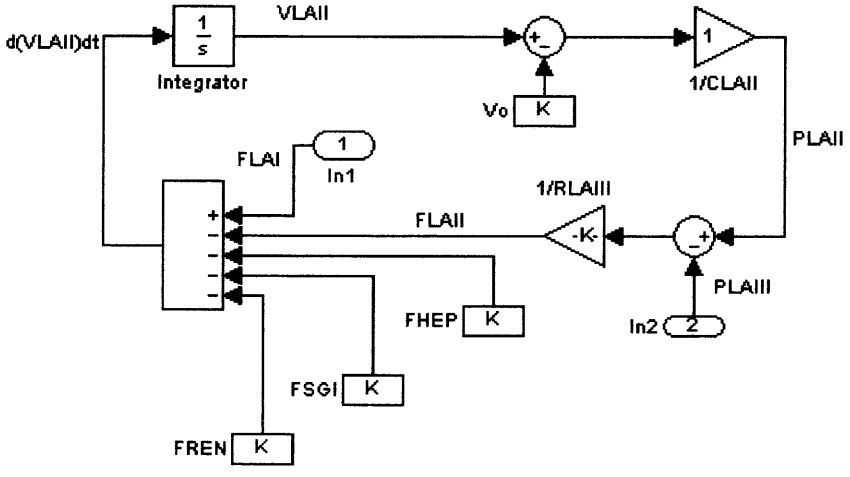

Figure B.2 Simulink realization for the Large Arteries II compartment of the model.

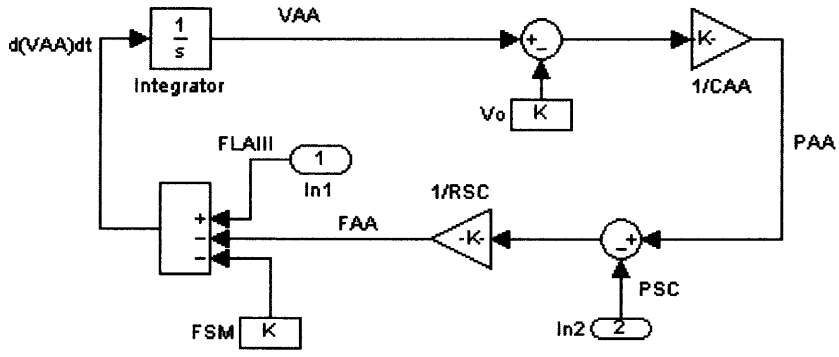

Figure B.3 Simulink realization for the Arterioles compartment of the model.

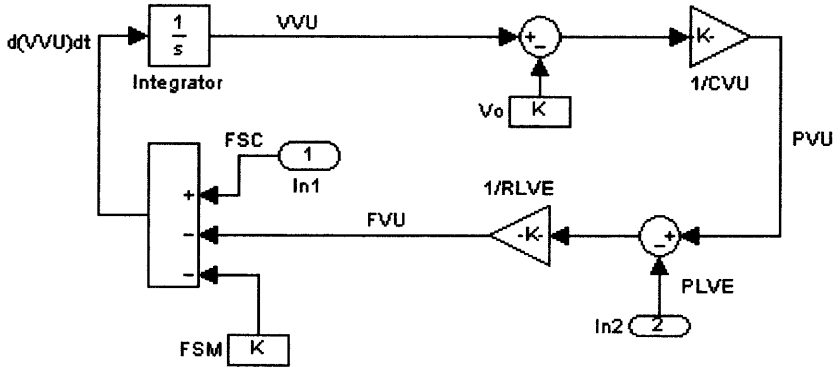

Figure B.4 Simulink realization for the Venules compartment of the model.

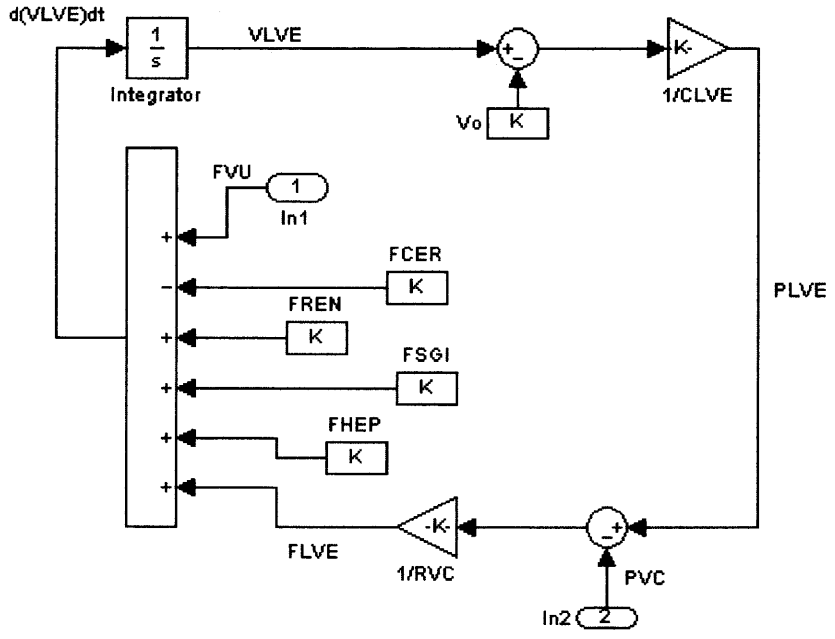

Figure B.5 Simulink realization for the Large Veins compartment of the model.

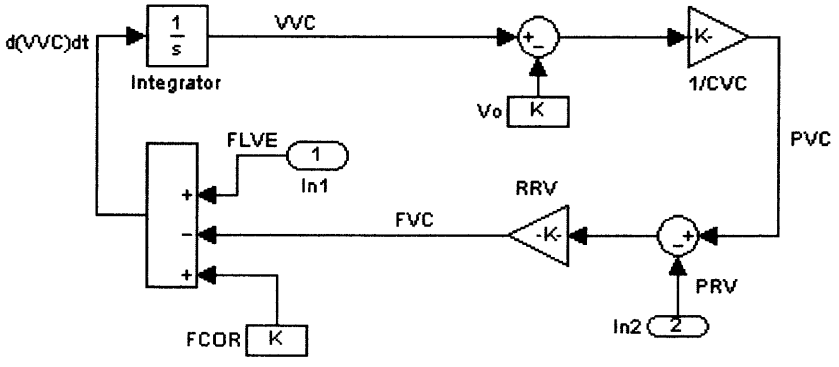

Figure B.6 Simulink realization for the Vena Cava compartment of the model.

APPENDIX C

WAVEFORMS GENERATED BY THE MODEL

The blood pressure and volume waveforms of the various compartments in the model generated by simulation are as shown from Figures C.1 to C.13.

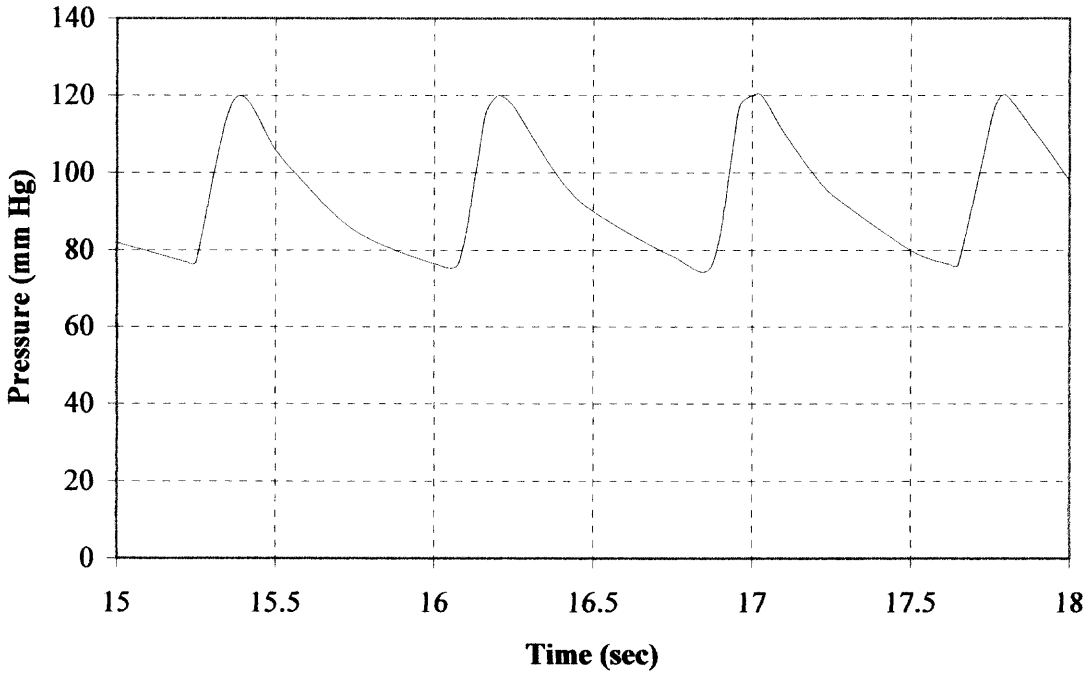

Figure C.1 Blood pressure in the Aorta generated by simulation.

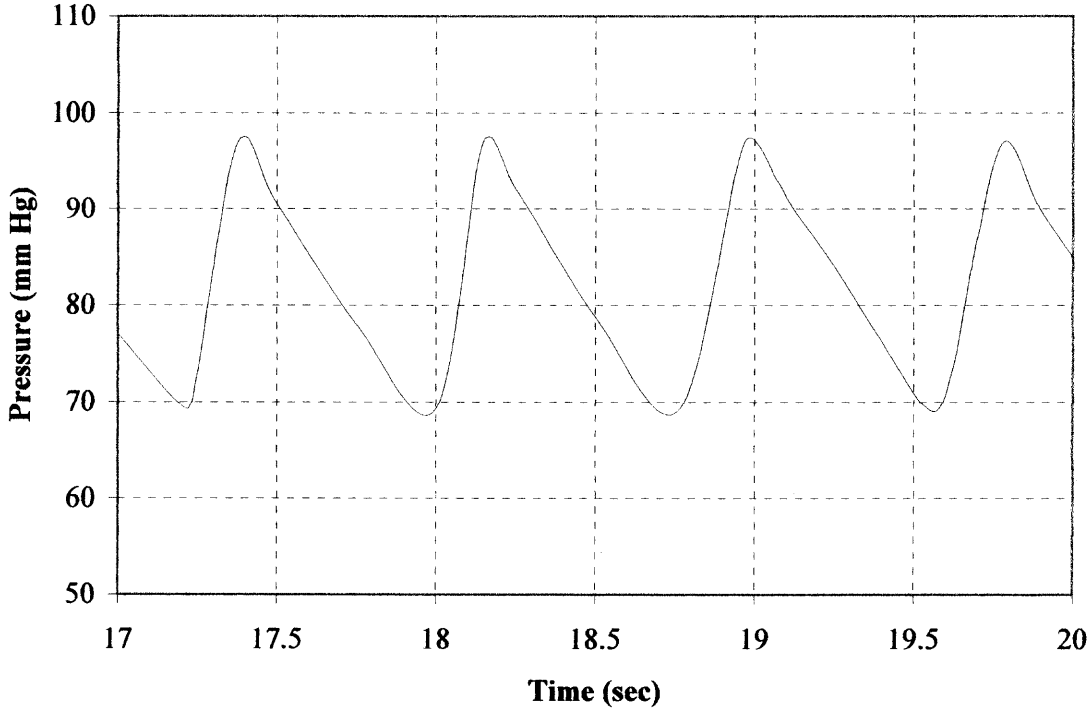

Figure C.2 Blood pressure in the Large Arteries generated by simulation.

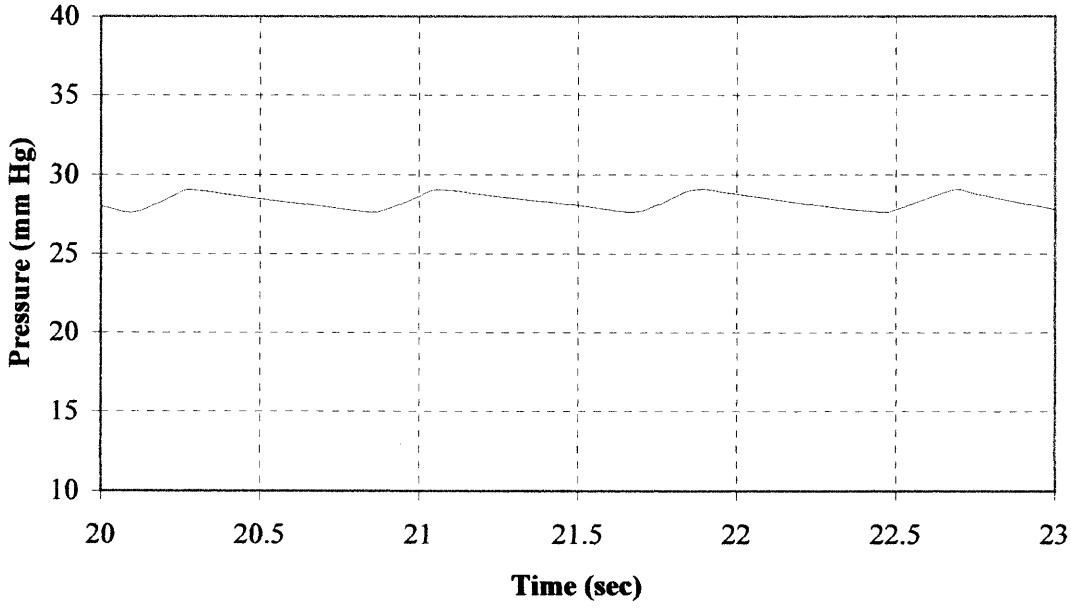

Figure C.3 Blood pressure in the Arterioles generated by simulation.

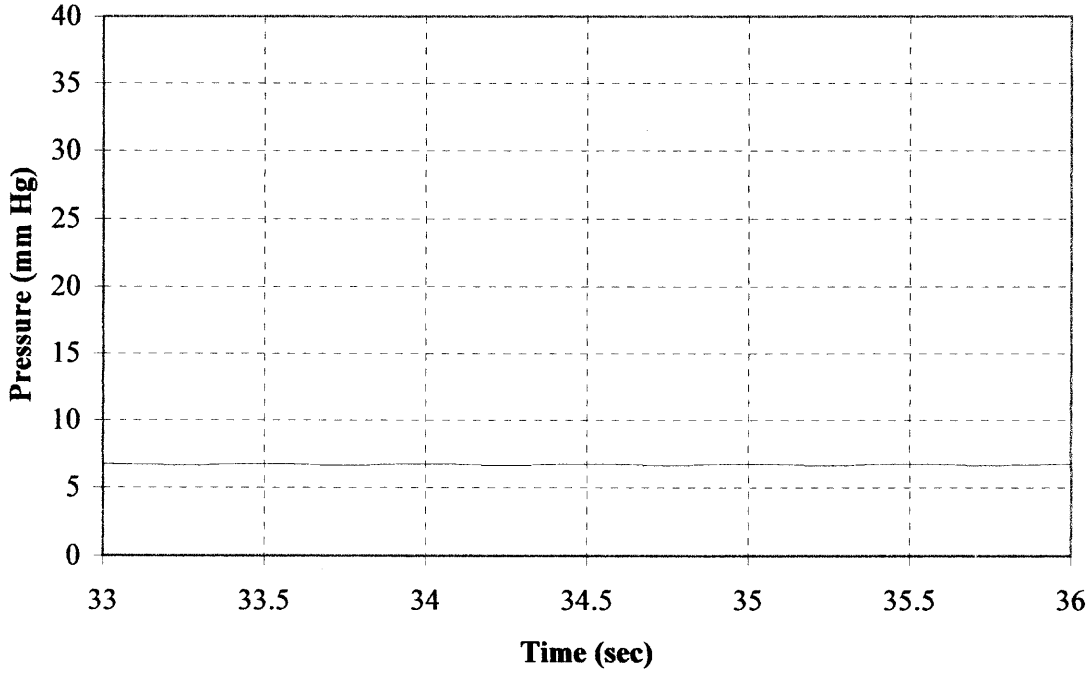

Figure C.4 Blood pressure in the Large Veins generated by simulation.

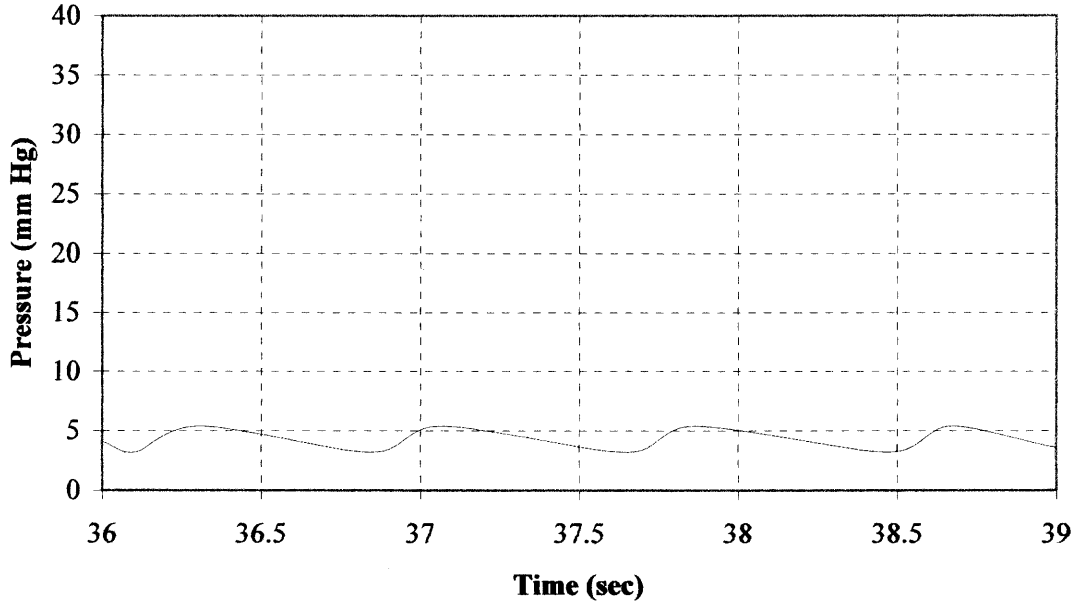

Figure C.5 Blood pressure in the Vena Cava generated by simulation.

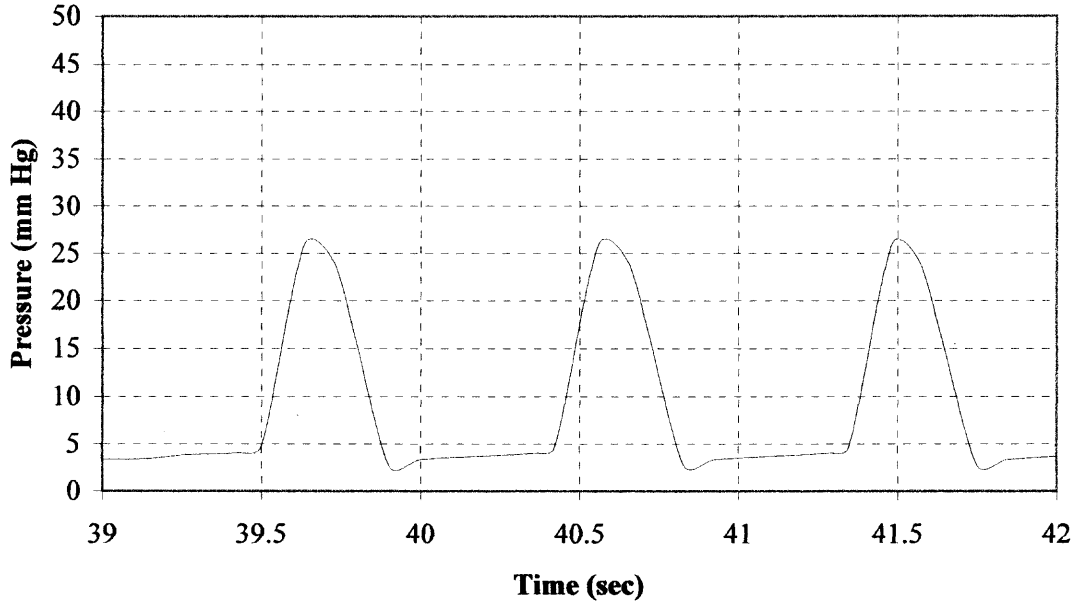

Figure C.6 Blood pressure in the Right Ventricle generated by simulation.

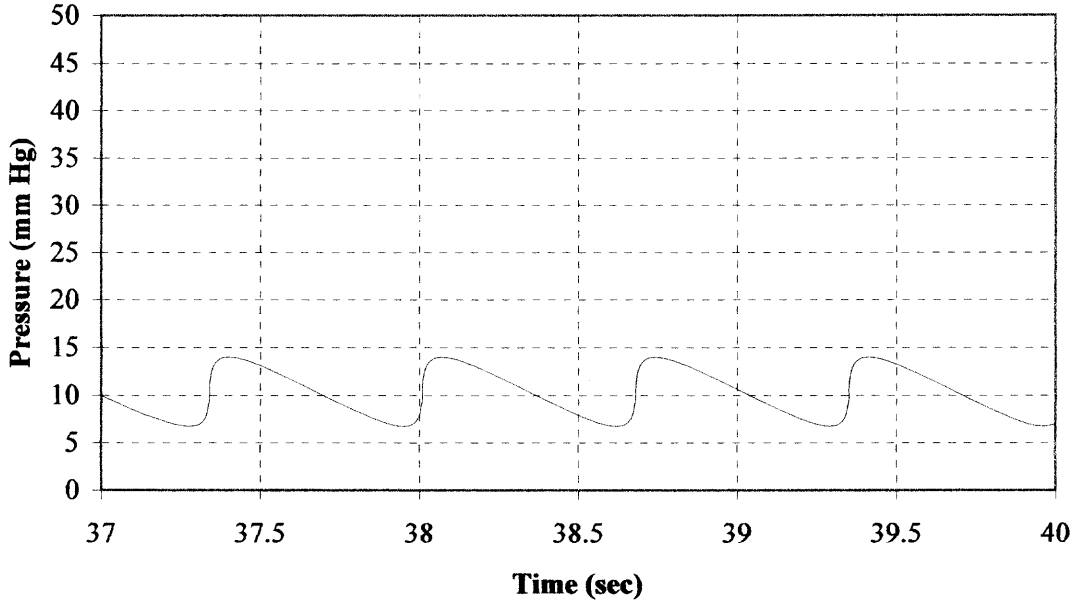

Figure C.7 Blood pressure in the Pulmonary Arteries generated by simulation.

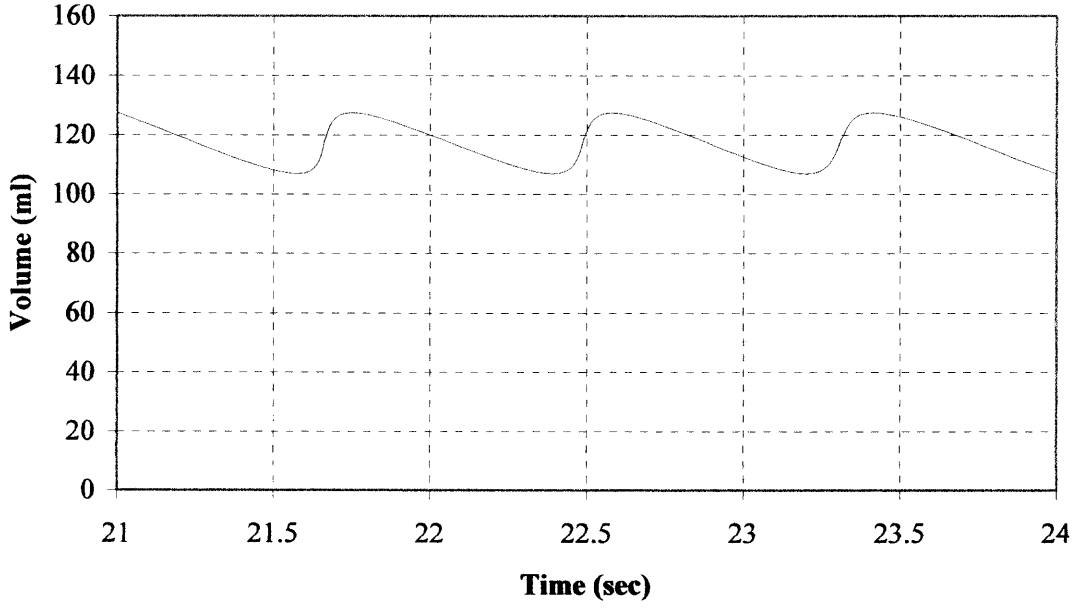

Figure C.8 Blood volume of the Large Arteries generated by simulation.

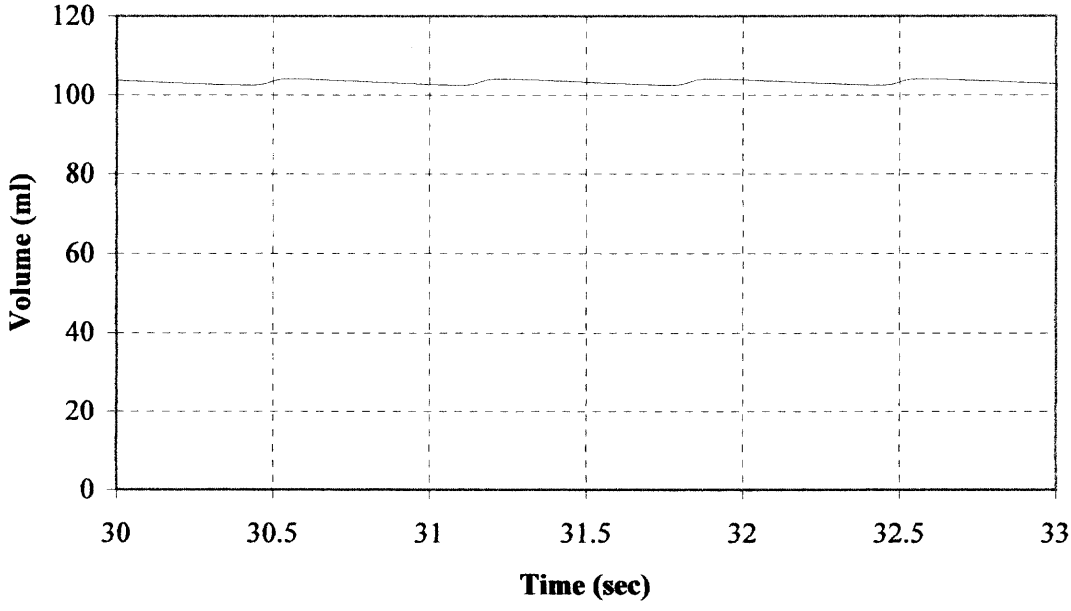

Figure C.9 Blood volume of the Arterioles generated by simulation.

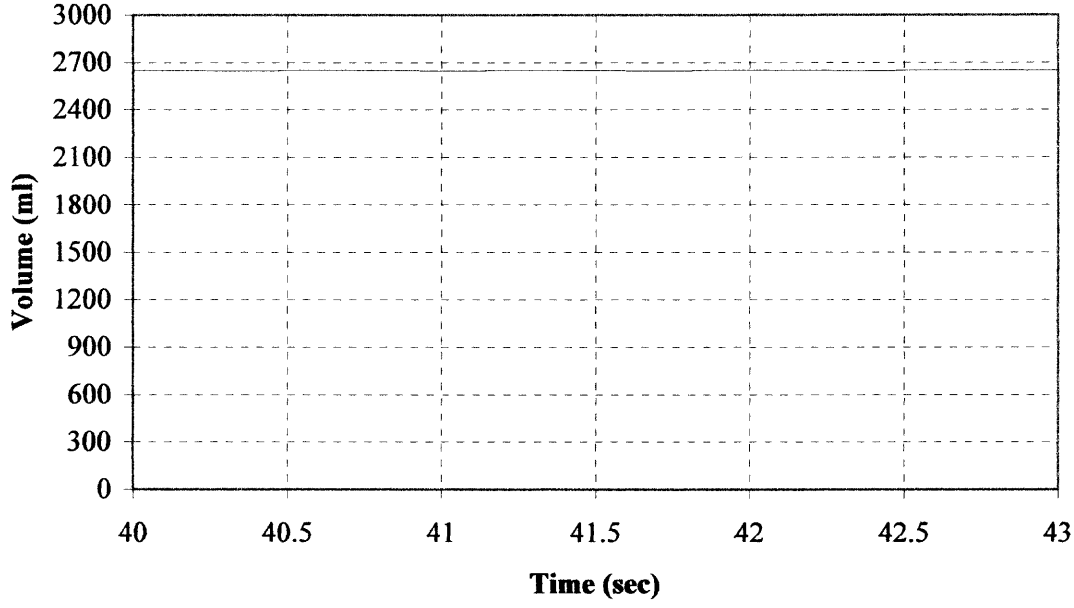

Figure C.10 Blood volume of the Large Veins generated by simulation.

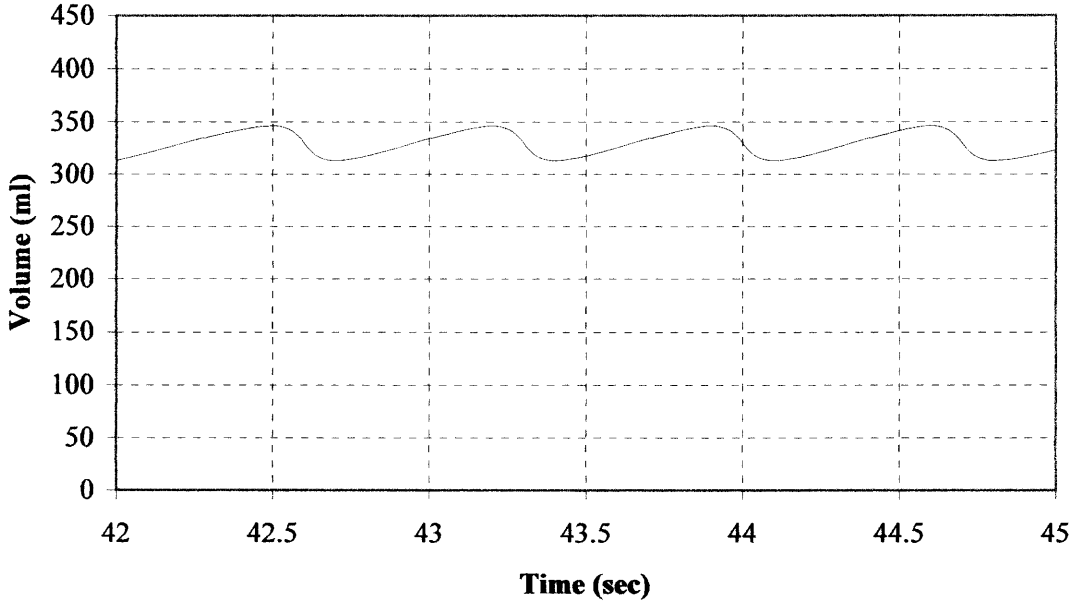

Figure C.11 Blood volume of the Vena Cava generated by simulation.

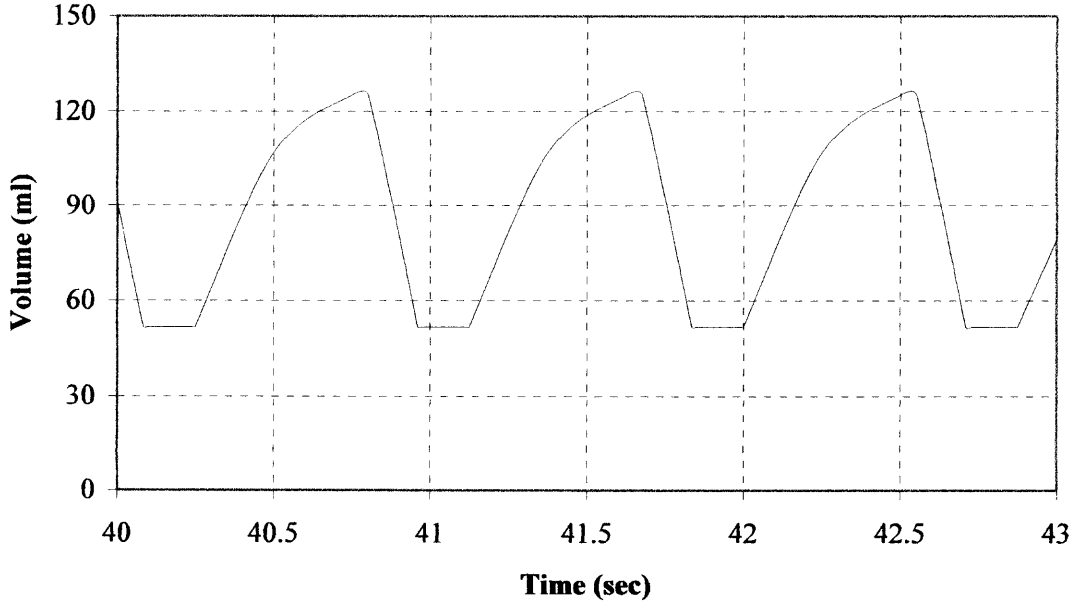

Figure C.12 Blood volume of the Right Ventricle generated by simulation.

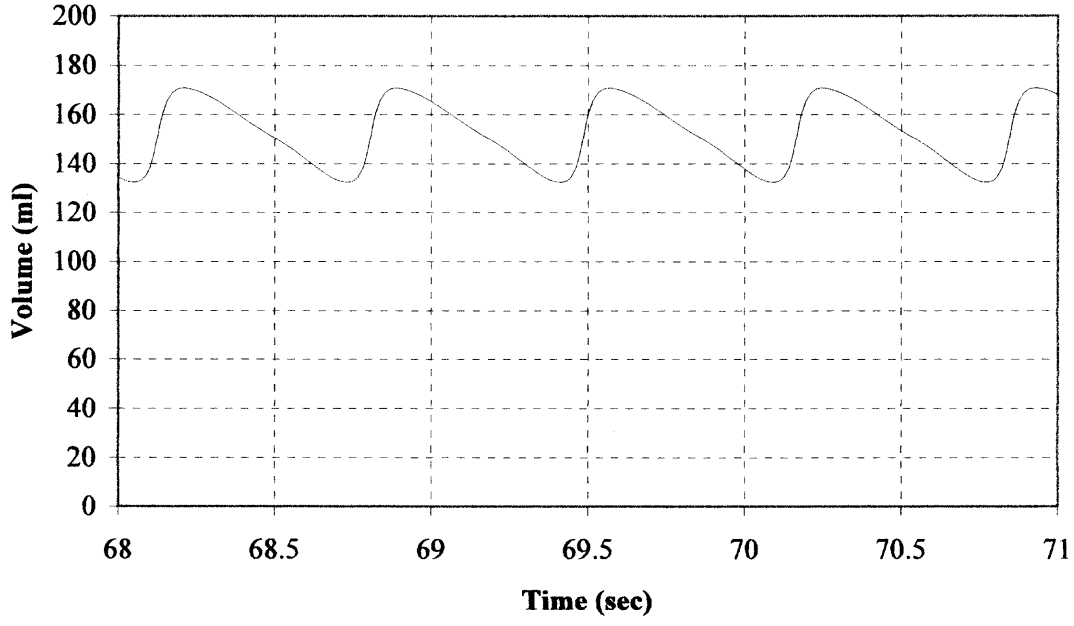

Figure C.13 Blood volume of the Pulmonary Arteries generated by simulation.

REFERENCES

1. Suga, H., and Sagawa, K. Instantaneous pressure-volume relationships and their ratio in the excised, supported canine left ventricle. *Cir. Res.* 35:117-126 (1974).

2. Shroff, S. G., Janicki, J. S. and Weber, K. T. Left ventricular systolic dynamic terms of its chamber mechanical properties. *Am. J. Physiol.* 245:H110-124 (1983).

3. Barnea, O. Mathematical analysis of coronary autoregulation and vascular reserve in closed-loop circulation. *Comput. & Biomed. Res.*, 27:263-275 (1994).

4. Ottensen, J. T. Modelling the dynamical baroreflex-feedback control. *Mathematical and Computer Modeling,* 31:167-173 (2000).

5. Brown, A. Receptors under pressure: An update on baroreceptors. *Circulation Research,* 46 (1980).

6. Suga, H. Controls of ventricular contractility assessed by pressure-volume ratio. *Cardiovascular Research,* 10 (1976).

7. Suga, H., Sugawa, K., and Kostiuk, D. P. Control of ventricular contractility assessed by pressure-volume ratio. *Critical Reviews in Biomedical Engineering.* (1976).

8. Sunagawa, K. Models of ventricular contraction based on time-varying elastance. *Critical Reviews in Biomedical Engineering.* (1982).

9. Eckberg, D. L. Nonlinearities of human carotid baroreceptor-cardiac reflex. *Circulation Research,* 47 (1980).

10. Levy, M. N., and Zieske, H. Autonomic control of cardiac pacemaker. *Journal of Applied Physiology,* 27 (1969).

11. Spickler, J. W., Kezdi, P., and Geller, E. Transfer characteristics of the carotid sinus pressure control system. *Baroreceptors and Hypertension,* 31-40. Pergamon Press, Dayton, OH (1965).

12. Wesseling, K. H., and Settels, J. J. Circulatory model of baro- and cardio-pulmonary reflexes. *Blood Pressure and Variability,* 56-67 (1992).

13. Warner, H. R., and Cox, A. A mathematical model of the heart rate control by sympathetic and vagus efferent information. *Journal of Applied Physiology,* 17:349-355 (1962).

14. Katona, P. G., and Barnett, G. O. Central origin of asymmetry in the carotid sinus reflex. *Annals New York Academy of Sciences,* 156:779-786 (1969).

15. Katona, P. G., Poitras, J. W., Barnett, G. O., and Terry, B. S. Cardiac vagal efferent activity and heart period in the carotid sinus reflex. *American Journal of Physiology,* 218:1030-1037 (1970).

16. Kezdi, P., and Geller, E. Baroreceptor control of postganglionic sympathetic nerve discharge. *American Journal of Physiology,* 214:427-435 (1968).

17. Olansen, J. B., Clark, J. W., Khoury, D., Ghorbel, F., and Bidani, A. A closed- loop model of the canine cardiovascular system that includes ventricular interaction. *Computers and Biomedical Research,* 33:260-295 (2000).

18. Takaoka, H., Takeuchi, M., Odake, M., Hayashi, Y., Hata, K., Mori, M., and Yokoyama, M. Comparison of hemodynamic determinants for myocardial oxygen consumption under different contractile states in human ventricle. *Circulation,* 87:59-69 (1993).

19. Suga, H., Yasumura, Y., Nozawa, T., Futaki, S., Igarashi, Y., and Goto, Y. Prospectice prediction of O_2 consumption from pressure-volume area in dog hearts. *American Journal of Physiology*, 252:H1258-H1264 (1987).

20. Guyton, A. C., and Hall, J. E. *Textbook of Medical Physiology*, W. B. Saunders Company, Pennsylvania (2000).

21. Melbin, J., Detweiler, D. K., Riffle, R. A., and Noordergraaf, A. Coherence of cardiac output with rate changes. *American Journal of Physiology*, 243:H499-H504 (1982).

22. Vander, A., Sherman, J., and Luciano, D. *Human Physiology: The Mechanisms of Body Function*, McGraw Hill, New York (2001).